

CHAPTER III

PHOTOELECTROCHEMICAL REACTIONS WITH SEMICONDUCTORS

3.1 Introduction of Semiconductors

The electronic properties of solids are usually described in terms of the band model,⁽⁹⁾ in which the behavior of an electron moving in the field of the atomic nuclei and all of the other electrons is treated. Consider the formation of a lattice of a solid (e.g. Cu, Si, TiO_2). The isolated atoms which are characterized by filled and vacant orbitals, when these orbitals are closely spaced that they form essentially continuous bands. They are depicted in Figure 3.1, one of the lower, or valence band which results from the overlap of filled valence orbitals of the individual atoms and the upper, or conduction band which results from overlap of empty higher orbitals of the atoms involved. These bands are separated by a forbidden region or band gap of energy E_g , which is usually given in units of electron volts, eV. The band pictures of metals, insulators and semiconductors are in Figure 3.1 (a), (b) and (c) respectively. The metal (e.g. copper), showing an overlap between the valence and conduction band, will show metallic conduction. For E_g large, $E_g \gg kT$, the crystal will be an insulator and the small E_g is semiconductor crystal. There are two types of semiconductors, one is the intrinsic semiconductor and the other is the extrinsic semiconductor

3.1.1 Intrinsic Semiconductors

When $E_g \ll kT$ or when the conduction and valence bands overlap, the material is good conductor of electricity. Under these circumstances, there exist in the solid filled and vacant electronic energy

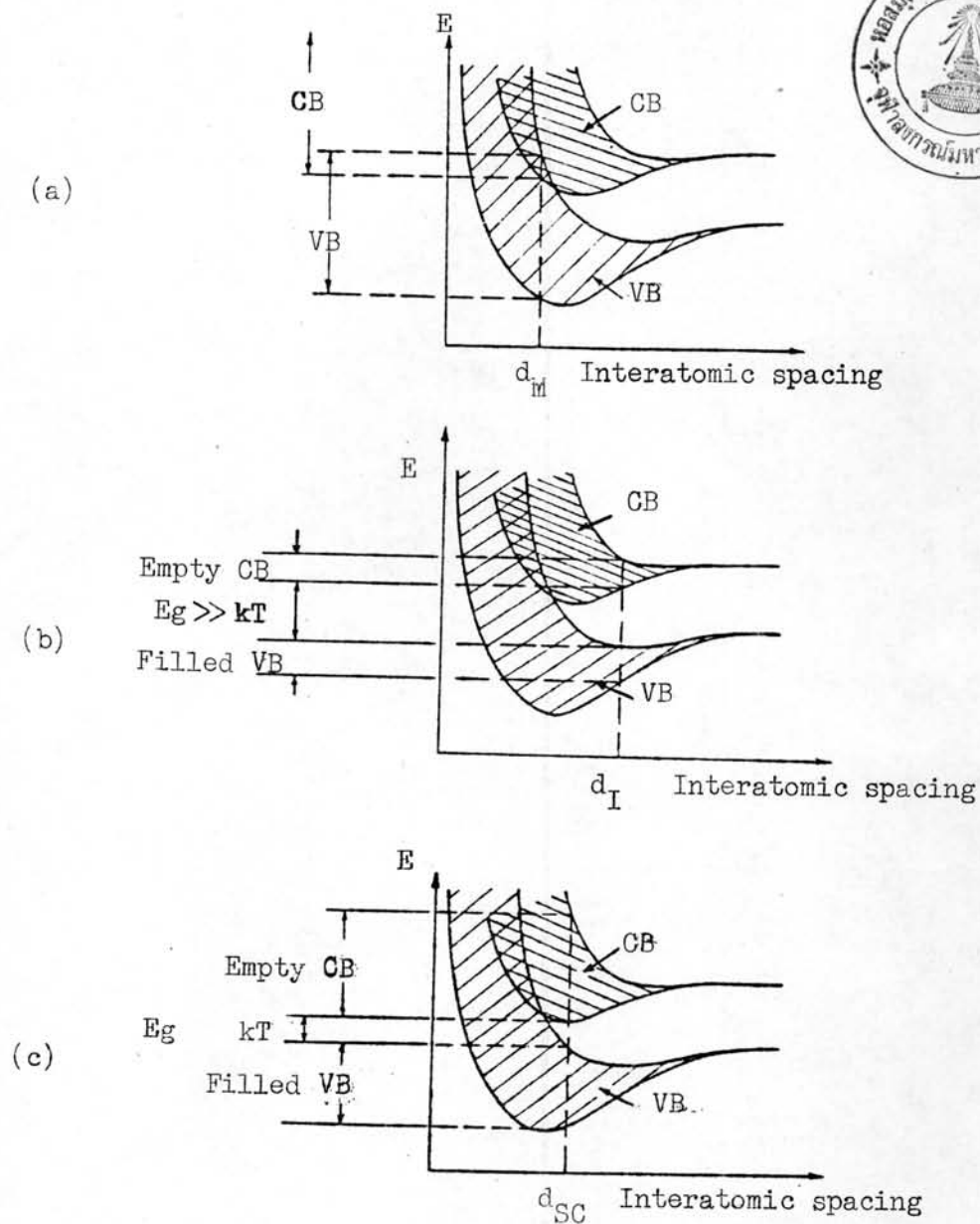


Figure 3.1 The band pictures of metal, insulator and semiconductor with interatomic spacing of d_M , d_I and d_{SE} respectively. For the room temperature, 27°C (300°K) kT is about 0.0259 eV .⁽⁹⁾

levels at the same energy, so that an electron can move from one level to another with only a small energy of activation. For small values of E_g (e.g. Si, where $E_g = 1.1$ eV), the valence band (VB) is almost filled and the conduction band (CB) almost vacant. The only carriers arise because of thermal excitation of electron from the VB into the CB (Figure 3.2). This process produces an electron in the CB, which is capable of moving freely to vacant levels in the CB, and leaves behind a hole in the VB that can be filled by VB electrons. Such a material is called an intrinsic semiconductor in which the density of CB electrons, n , and of VB holes, p , is given by the expression. (39)

$$n.p = n_i^2 = N_c N_v \exp(-E_g/kT) \text{ cm}^{-6} \quad \dots 3.1$$

For example, for Si (N_c and N_v are 1.04×10^{19} and $6.0 \times 10^{18} \text{ cm}^{-3}$ respectively) (39)

$$n = p = 1.45 \times 10^{10} \text{ cm}^{-3} \text{ (at } 27^\circ\text{C)}.$$

For materials with $E_g \sim 1.5$ eV, few carriers are produced by thermal excitation at room temperature that in the pure state such solids are electrical insulators (e.g. GaP and TiO_2) with E_g equal to 2.2 and 3.0 eV, respectively or semiconductors with large E_g .

3.1.2 Extrinsic Semiconductors

Electrons in the CB and holes in the VB can also be introduced by the addition of acceptor and donor species (called dopants) into the semiconductor. Thus arsenic (a group V element) behaves as an electron donor material when added to silicon (a group IV element) and introduces an energy level at E_D near (within ~ 0.05 eV) the bottom of the CB. At room temperature most of the donor atoms will be ionized, each one yielding CB electron and leaving behind isolated positive sites at the donor atom nuclei (Fig 3.3a). For example, if the amount of dopant

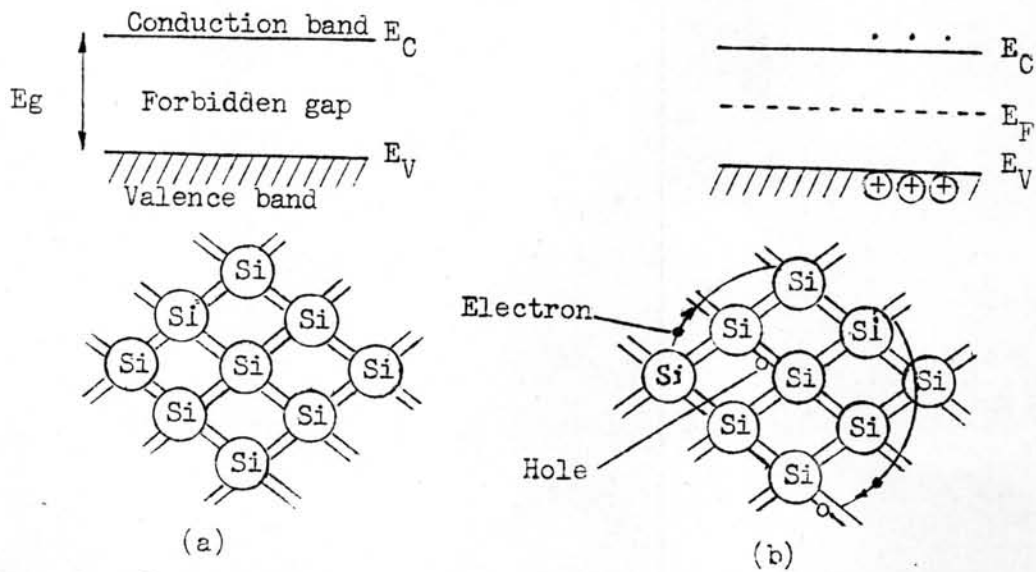


Figure 3.2 Energy bands and two-dimensional representation of an intrinsic semiconductor lattice.

- (a) At absolute zero (or $E_g \gg kT$), assuming a perfect lattice; no holes and electrons exist.
- (b) At a temperature where some lattice bonds are broken, yielding electrons in the conduction band and holes in valence band.

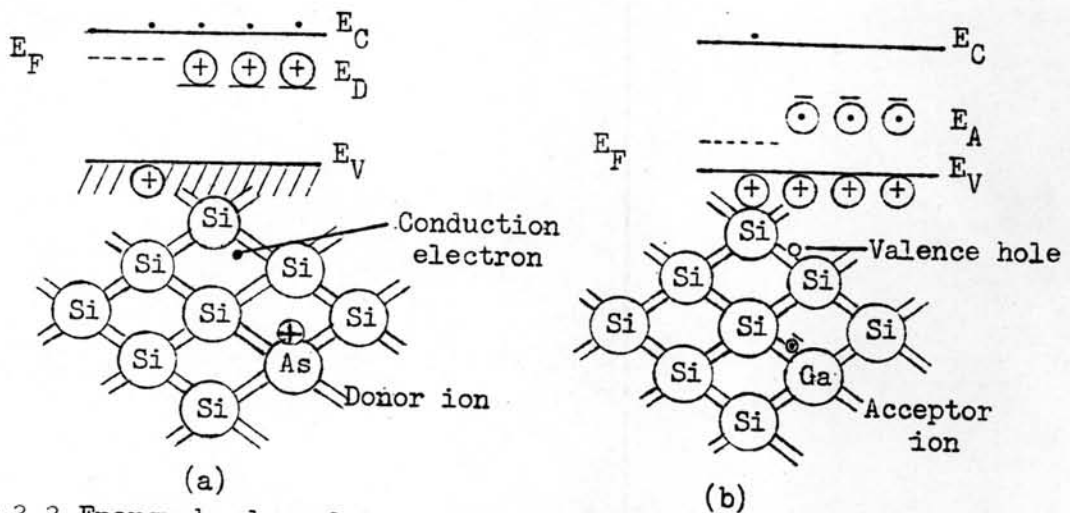


Figure 3.3 Energy bands and two-dimensional representation of the extrinsic semiconductor lattices.

- (a) n-type semiconductor
- (b) p-type semiconductor

is about 1 ppm, the donor density N_D will be $\sim 5 \times 10^{16} \text{ cm}^{-3}$, this will be the CB electron density n . The hole density p is much smaller and is given by $p = n_i^2/N_D$. Thus for this example of As-doped Si, $p \sim 4200 \text{ cm}^{-3}$ at 25°C. A material doped with donor atoms is called an n-type semiconductor.

If an acceptor element (e.g., gallium, a group III element) is added to the Si, an energy level at E_A near the top of the VB is introduced (Figure 3.3b). In this case electrons are thermally excited from the VB into these acceptor sites, leaving behind mobile holes in the VB with the formation of isolated negatively charged acceptor sites. Thus the acceptor density N_A of 5×10^{16} atoms of acceptor per cm^{-3} , is essentially the same as the hole density p . In this case the CB electron density n is given by $n = n_i^2/N_A$ or in the above example, $n \sim 4200 \text{ cm}^{-3}$. Thus, the holes are the majority carriers, the electrons are the minority carriers, and the material is called a p-type semiconductor.

An important concept in the **description** of semiconductor electrodes is that of the Fermi level, E_F , which is defined as that energy where the probability of a level being occupied by an electron is $\frac{1}{2}$, in other words where it is equally probable that the level is occupied or vacant (See 3.1.3). For an intrinsic semiconductor at room temperature, E_F lies essentially midway between the CB and VB within the forbidden gap region. Note that in contrast to metals, where both occupied and vacant states are present at an energy near E_F , for an intrinsic semiconductor neither electrons nor unfilled levels exist near E_F . For a doped material the location of E_F depends on the doping level, N_A or N_D ; for moderately or heavily doped n-type solid ($N_D > 10^{17} \text{ cm}^{-3}$), E_F lies slightly below the CB edge (Figure 3.3a)

3.1.3 Fermi-Dirac Distribution Function.

The energy distribution of electrons in a solid is governed by the laws of Fermi-Dirac statistics. The principal result of these statistics is the Fermi-Dirac distribution function which gives the probability that an electronic state which energy E is occupied by an electron,

$$f(E) = \left[1 + \exp(E - E_F)/kT \right]^{-1}$$

This function contains a parameter, E_F , which is called the Fermi level, is that energy at which the probability of occupation of an energy state by an electron is exactly one-half.

The Fermi-Dirac distribution function is illustrated in Fig.3.4a for the case of an intrinsic semiconductor. At the left side of this figure we show the probability of occupation of states by electrons as a function of the energy of the states. In the conduction band there are a large number of states, However, the probability of occupation of these state is small; hence, there will be only a few electrons in the conduction band. By contrast, there are also a large number of states in the valence band. Most of these are occupied by electrons since the probability of occupation of states there is nearly unity. Thus there will be only few unoccupied electron states, i.e., holes, in the valence band.

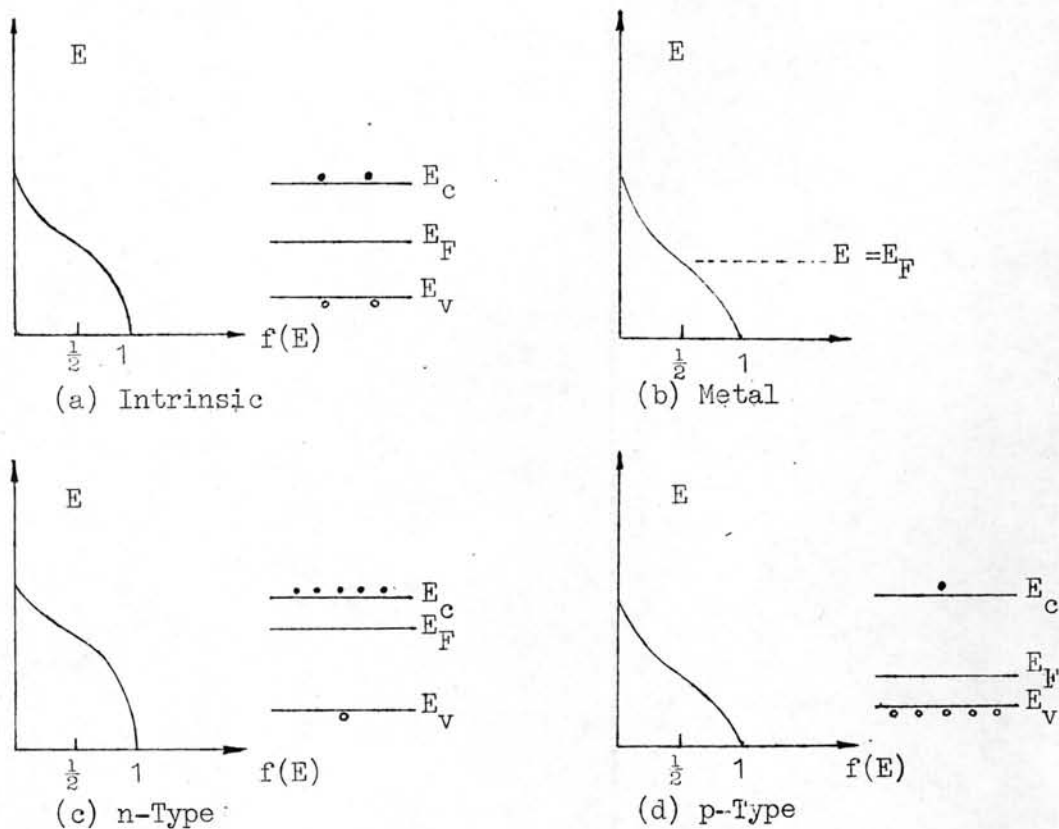


Figure 3.4 Illustration of the Fermi-Dirac distribution function for intrinsic, metal, n- and p-type semiconductor.⁽³⁹⁾

The Fermi-Dirac distribution function is symmetrical around the Fermi level E_F . Thus, if the number of energy states in the conduction and valence bands are the same, and if the number of electrons in the conduction band and the number of holes in the valence band are also the same, the Fermi level must be located in the middle of the energy gap. This is approximately what happens in an intrinsic semiconductor. For metallic conductors, Fig. 3.4b shows the electron energy levels as they might appear in a real metal in a typical Fermi distribution.

In an n-type semiconductor, the concentration of electrons in the conduction band is larger than in the intrinsic case. Since, however, the density of energy states in the conduction band is the same as in the intrinsic case, it follows that in an n-type semiconductor the Fermi level, and with it the entire Fermi-Dirac distribution, will be shifted upward in the energy-band picture. In contrast, in a p-type semiconductor the Fermi level and the Fermi-Dirac distribution function will both be shifted downward. These two cases are illustrated in Fig. 3.4 c and d.

3.1.4 The Maximum Useful Temperature for a Semiconductor Devices

When the working temperature of an extrinsic semiconductor is increased the number of thermally generated carrier pairs, (electron and hole contributed by the semiconductor atoms) increases to the point where they equal or exceed those contributed by the impurities (whose number is fixed). The semiconductor then loses its extrinsic nature and becomes intrinsic, since the concentrations of electrons and holes become about equal. Semiconductor-device operation is always based on its being n-or p-type or n in some region p in others. The intrinsic temperature, marked T_{max} , is therefore the absolute maximum for any semiconductor device and in fact one should stay well below it. Taking N-type, for example, we get T_{max} from the condition $n_i \approx N_D$, Using Eq.3.1, this condition gives.

$$n_i = (N_C N_V)^{\frac{1}{2}} \exp(-E_g/2k T_{max}) = N_D \quad \dots 3.2$$

$$T_{max} = E_g/2k \ln \left[(N_C N_V)^{\frac{1}{2}} / N_D \right] \quad \dots 3.3$$

For Si, at a doping level of $N_D = 5 \times 10^{14} \text{ cm}^{-3}$, this gives $T_{max} \approx 660\text{K}$,
287°C



For Ge, with small E_g , T_{max} is about 170°C . These numbers are reduced for lower doping. A practical maximum working temperature for Ge device is around 90°C and for Si it is around 200°C ⁽⁴⁾, but it may be limited by the manufacturer. It is obvious from Eq. 3.3 that the higher E_g is, the better the semiconductor is for high-power (and therefore high-temperature) operation. For a solar cell, this is one of the main reasons for silicon replacing germanium and for the interest in developing GaAs devices with still higher E_g .

3.1.5 Light -Semiconductor Interactions

Interaction between electromagnetic light photons and a semiconductor means that the photons are either absorbed or emitted by the semiconductor. Appreciable, and therefore useful, absorption results from the generation of hole-electron pairs. This puts an upper bound on λ to which a specific semiconductor can react, which is the wavelength of which the photon energy equal the band gap. At longer λ the semiconductor become transparent, or almost so, and can no longer be used with that light.

The energy E of the photon is related to its wavelength λ by

$$E = h\nu = hc / \lambda = 1.24 / \lambda \quad \text{eV} \quad \dots 3.4$$

Equating E to the band gap E_g yields the maximum useful wavelength :

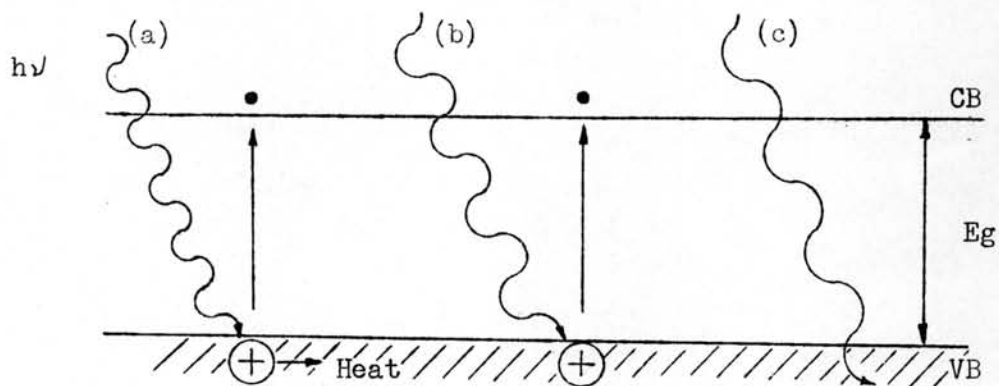
$$\lambda_{max} = 1.24 / E_g \text{ (eV)} \quad \mu\text{m} \quad \dots 3.5$$

Table 3.1.4 Lists λ_{max} for some useful semiconductors. As E_g usually becomes smaller with increasing temperature, it is important to list the operating temperature too. And Fig. 3.5 shows that the absorption result forming the generation of hole-electron pair

Table 3.1.4⁽⁴⁾ Working temperatures of semiconductors

Semiconductor material	λ_{\max} (μm)	Working Temperature, K
ZnS	0.35	300
CdS	0.52	300
GaP	0.55	300
GaAs	0.88	300
Si	1.2	300
Ge	1.8	300
InAs	3.0	77
InSb	5.5	77

Fig.3.5 A Light photon of proper wavelength (b) creates a hole- electron pair. Photons of the shorter wavelength (a) creates a pair as well as heat while the longer wavelength photons (c) pass through the semiconductors.



The working temperature is determined by a very important consideration: carriers are continuously generated by thermal energy as well as by

incoming light. Thermal generation must therefore be made much smaller than that caused by the absorbed photons for the latter to be noticeable. But the longer λ is the lower must E_g be, and consequently the higher n_i becomes, which represents thermal generation (Eq. 3.1 predicts exponential dependence for n_i on E_g). In InSb, for example, the band gap is 0.18 eV at 300°K, which makes n_i so high that it behaves like a good conductor even without intentional doping or the addition of light-generated carriers. On cooling it to 77°K (with liquid nitrogen), E_g is increased to 0.23 eV and n_i is decreased by 10^{-6} approximately. Optically generated carriers will now have a strong effect on the conductivity and can therefore be detected. The longer the wavelength the lower the working temperature must be, as can be seen from Table 3.1.4.

Optical irradiation, absorption and carrier generation can be related as follows: suppose the semiconductor is irradiated by P watts per unit area of optical energy. If the radiation is monochromatic, the photon flux ϕ_0 hitting a unit area per unit time is obtained by dividing P by the energy of a single photon E_{ph} :

$$\phi_0 = P/E_{ph} = P/h\nu = P\lambda/hc \quad \dots 3.6$$

This means that for a constant P , ϕ_0 grows linearly with λ . If no special antireflection coating is used, only a fraction $\eta(\lambda)$ of these photons will penetrate the semiconductor and be absorbed. The rest are reflected at the semiconductor-air interface because of the difference in refractive indices. An antireflection coating is used to minimize the reflection, making $\eta(\lambda) \approx 1$ there.

Let X represent the depth into the semiconductor from its irradiated surface and $\phi(X)$ the photon flux at this depth. The carrier generation,

$g(x)$ at depth x must equal the change of $\phi(x)$ with x on one hand and be proportional to $\phi(x)$ on the other:

$$g(x) = -d\phi / dx = \alpha(\lambda) \phi(x) \quad \dots 3.7$$

The proportionality constant, $\alpha(\lambda) (\text{cm}^{-1})$ is called the absorption coefficient and depends on the material and on λ .

The solution to this equation is:

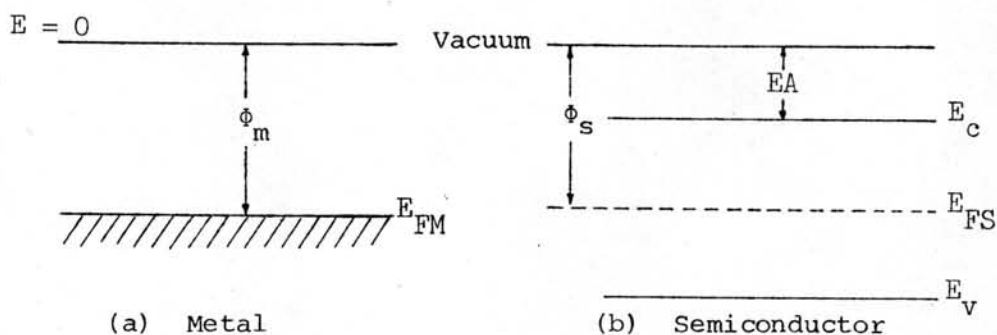
$$\phi(x) = \eta\phi_0 \exp(-\alpha x) \quad \dots 3.8$$

since $\phi = \eta\phi_0$ at $x = 0$ By substituting Eg.3.8 into Eg.3.7, then $g(x) = \eta\alpha\phi_0 \exp(-\alpha x)$, is strongest near the surface and decays exponentially with x .

3.2 Metal-Semiconductor Junction

One important junction form being necessary to use for solar cell and photoelectrode in photoelectrochemical cell is the metal-semiconductor junction. From Appendix A.2, the p-n junction is the main part which electrical energy is generated and pass passes through the metal semiconductor junction to external circuit for load.

There are two types of this junction, their junction forms depend on work function of metal and semiconductor using for junction forming. The work function is the energy supply to an electron in the fermi level (see 3.1) of metal or semiconductor (Figure 3.2.1) for being the free electron in a vacuum ($E = 0$). Some values for the work function, ϕ of metals and semiconductors is in Table 3.2.1.



Figar.3.2.1 Relationships between energy levels and ϕ (work function) and EA (electron affinity) for (a) metal; (b) semiconductor.

Table 3.2.1 Work function of metals and semiconductors ⁽¹⁴⁾

Metal or Semiconductor	Work function ϕ , eV
Ag	4.73
Al	4.08
Au	4.82
Cu	4.38
In	3.79
Pb	4.00
Zn	4.00
Pt	5.32
Ge	4.3
Si	3.6
TiO ₂	~ 5.5 ⁽³¹⁾

3.2.1 Schottky Junction

In this case, the work function of metal, ϕ_m , is larger than the work function of semiconductor, ϕ_s . Consider an interface formed

by contacting together an n-type of semiconductor and a metal. Before the junction is formed (Figure 3.2.2a), there is overall electroneutrality in both types of material. The charge carrier in the n-type of material will be mostly electrons. Thus, in the containing, electrons in the semiconductor diffuse into metal side.

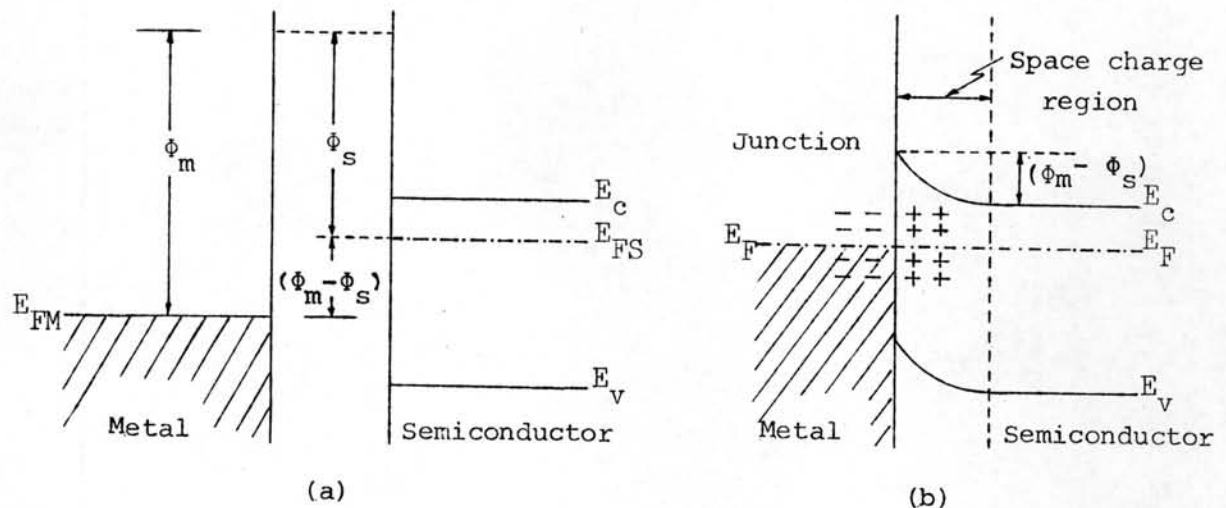


Figure 3.2.2 Representation of the formation of the junction between metal and n-type semiconductor ($\phi_m > \phi_s$) (a) before contact (b) after contact at equilibrium (the location of E_{FM} is shifted up to the level of E_{FS}).

The equilibrium is reached when the driving force for the diffusion (the concentration gradient) is just compensated for by the electric field (the potential gradient), like the p-n junction phenomena in Appendix A.1. Under this equilibrium (Figure 3.2.2b), the positive charges of the immobile donors in the n-type of material exactly balances the negative charges of the free electrons in the metal side; no electrons diffuse to pass the region (which the band level bend up because of the potential is positive with respect to the bulk), there is a barrier potential, corresponding to $\phi_m - \phi_s$. This region is a space charge region (cf. p-n junction).

Under forward-bias condition (in which a negative voltage is applied to n-type region relative to the metal), the barrier potential across the junction is smaller than in equilibrium, bringing about a narrowing of the space-charge region. Therefore, electrons can diffuse through the junction, in this condition large currents flow across the junction too. It is a rectifier by forward-bias the junction, as p-n junction (see Appendix A.1). This junction is called Schottky junction or schottky diodes e.g. Al-nSi, Sn-pSi etc., as a kind of solar cells.

In photoelectrochemical cells, the interface of semiconductor electrode and electrolyte (O/R substant) is behavior like the Schottky junction, will be discussed in 3.4.2.

3.2.2 Ohmic Junction

In this case $\phi_m < \phi_s$ (Figure.3.2.3 a), the E_{FM} is located at the higher than E_{FS} , thus electrons in the metal can diffuse into n-type semiconductor when in contact face to face unit . . . equilibrium, and the phenomena is also like that in the case of $\phi > \phi$ but in opposite direction (Figure 3.2.3 b)

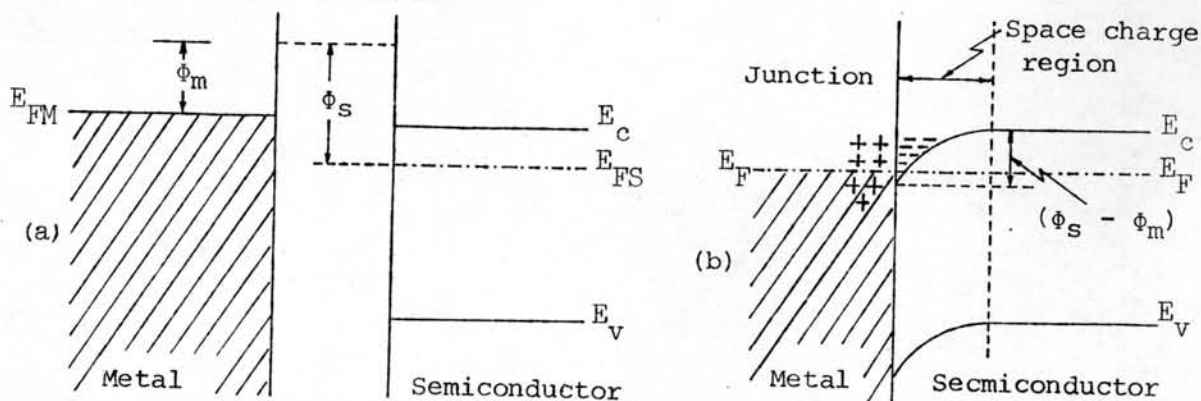


Figure 3.2.3 Representation of the formation of the junction between metal and n-type semiconductor ($\phi_m < \phi_s$) (a) before contact (b) after contact at equilibrium. Thus, near the surface the band bend down, and

no barrier potential for blocking the electrons across the junction. This junction is called ohmic junction, it is used for the connection of solar cell (p-n junction) and the conducting wire. In the same way, the photoelectrode and conducting wire connection must be the ohmic contact also. For the TiO_2 photoelectrode (ϕ is ~ 5.5 eV), the suitable material is In (ϕ is 3.79 eV). Some papers, they used the alloy of Ga-Ag⁽⁴⁵⁾ or Ga-In⁽⁴⁸⁾

To study the metal-semiconductor junction, we will introduce the process of reactions at semiconductor electrode in a photoelectrochemical cell, and give the information on the suitable material for connection of electrode and conducting wire.

3.3 Semiconductor Electrodes

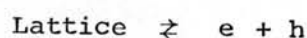
Only a very limited number of electrode materials can be used for photoelectrochemical cells. The materials which have the property of storing light energy for a time long enough to be converted into another forms of energy, and a low enough inner resistance to avoid high energy losses during the flow of an electric current are semiconductors

The basic properties of these materials (see 3.1) have to be well understood in order to discuss the mechanisms of such cells in this section.

3.3.1 Some Analogies between Semiconductors and Electrolytic Solution

In semiconductors, the electrons of valence band are used for bonding together atoms, the removal of a valence electron by excitation into the conduction band implies the rupture of a bond in the lattice. The creation of an electron-hole pair may therefore be treated as an

ionization reaction



and the ionization of water in an electrolytic solution is



Both equilibrium reactions can be treated by the law of mass action. Just as the product of the concentrations of hydroxyl ions and hydrogen ions remains a constant at a fixed temperature,

$$C_{\text{H}^+} \times C_{\text{OH}^-} = K_{\text{H}_2\text{O}}$$

the product of the electron n and hole p concentrations also remains a constant at fixed temperature. The constant depends on the energy gap E_g across which the valence electrons must be excited into the conduction band

$$np = K_{\text{SC}}$$

where K_{SC} is a constant characteristic of the intrinsic semiconductor or is n_i^2 for Eq.3.1. Further, just as, in pure water, the concentrations of hydroxyl (OH^-) and hydrogen ions (H^+) are equal, the electron and hole concentrations in an intrinsic semiconductor are equal

$$n = p = K_{\text{SC}} = n_i$$

There are remarkable parallels between the ionization of the lattice of an intrinsic semiconductor and ionization of water, shown in Table 3.3.1

3.3.2 The Semiconductor-electrolyte Interface

The electrode-solution interface has been shown experimentally to behave like a capacitor, and a model of the interfacial region somewhat resembling a capacitor can be given. From Figure 3.3.2 a, there are two important layers of ions in the solution side and the second row is

Table 3.3.1

Some Analogies between Semiconductors and Electrolyte Solutions⁽⁹⁾

This phenomenon	in aqueous solution	in a semiconductor
Dissociation of solvent Law of mass action	$\text{H}_2\text{O} \rightleftharpoons \text{H}^+ + \text{OH}^-$ $(\text{H}^+)(\text{OH}^-) = K_w$ $n_{\text{H}^+} = n_{\text{OH}^-} \approx 10^{14} \text{ ions cm}^{-3}$	$\text{Lattice} \rightleftharpoons e^- + p^+$ $np = ni^2$ $n = p \approx 10^{15} - 10^{16} \text{ cm}^{-3}$
Behavior of acid	$\text{HCl} \rightleftharpoons \text{H}^+ + \text{Cl}^-$ <p>proton donor</p>	$\text{As} \rightleftharpoons \text{Electron} + \text{As}^+$ <p>electron donor</p>
Behavior of base	$\text{NH}_3 + \text{H}^+ \rightleftharpoons \text{NH}_4^+$ <p>(proton acceptor)</p>	$\text{Ga} + e^- \rightleftharpoons \text{Ga}^-$ <p>(electron acceptor)</p>
Common-ion effect	<p>(a) Adding acid (proton donor) to water increases proton concentrations</p> <p>(b) Adding base (proton acceptor) to water decreases proton concentration and increases OH^- concentration</p>	<p>(a) Adding electron donor to intrinsic semiconductor increases electron concentration</p> <p>(b) Adding electron acceptor to semiconductor decreases electron concentration and increases hole concentration.</p>

largely reserved for solvated ions is called the outer Helmholtz plane (OHP).^(6,9)

Using Semiconductor as an electrode in an electrolytic cell a variable electric charge can be also accumulated in a space charge region underneath the interface with electrolyte, and at equilibrium the interface behaves like a capacitor as Fig.3.3.2. (cf. p.n. Junction in Appendix A.1). For example, using n-type semiconductor electrode in the solution electrons will flow from the semiconductor (which becomes positively charged) to the solution (which becomes negatively charged). At equilibrium, the positive charge on the semiconductors exactly balances the negative charge of the double layer of OHP in the solution. As a consequence, the electrical field and barrier potential is established, charge carrier concentrations and potential values of the band edges differs between bulk and surface of the semiconductor (Figure 3.3.3b and b.), and is represented by a bending of the band. The band is bent upward (with respect to the level in the bulk semiconductor) when the semiconductor charge is positive with respect to the solution.

Bockris and Reddy⁽⁹⁾ demonstrated the potential profile inside semiconductor by the Gony-Chapman theory of the diffuse layer.

$$\phi_x = \phi_s e^{-\kappa x}$$

where ϕ_x and ϕ_s are potential at distance x and potential at the surface respectively and

$$\kappa = \left(\frac{8\pi n_0 q^2}{\epsilon kT} \right) \text{ cm}^{-1}$$

where n_0 , q , ϵ , k and T were density of electrons, electronic charge, dielectric constant of the medium, the Boltzmann constant and absolute

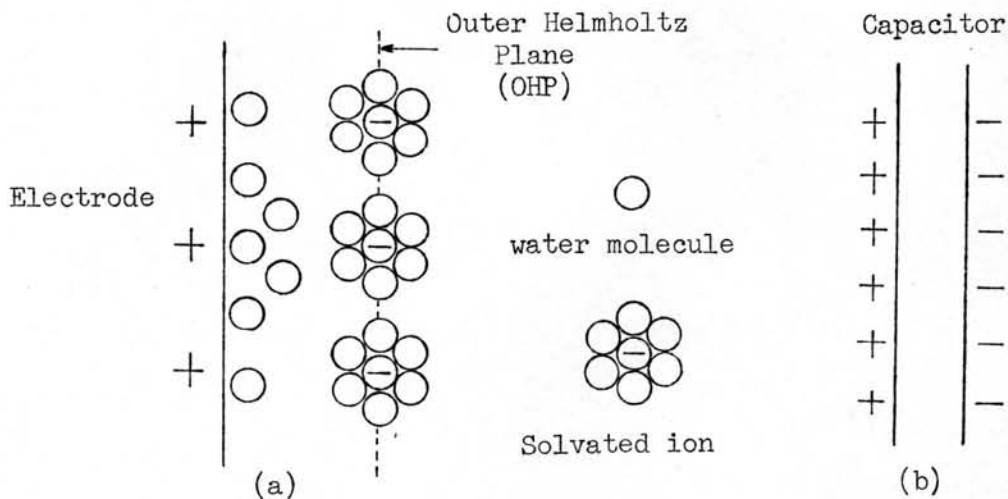


Figure 3.3.2 (a) A double layer, the water molecule is in the first row and the locus of centers of these solvated ions is defined the OHP. (b) The electrical equivalent of such a double layer is a parallel-plate capacitor.

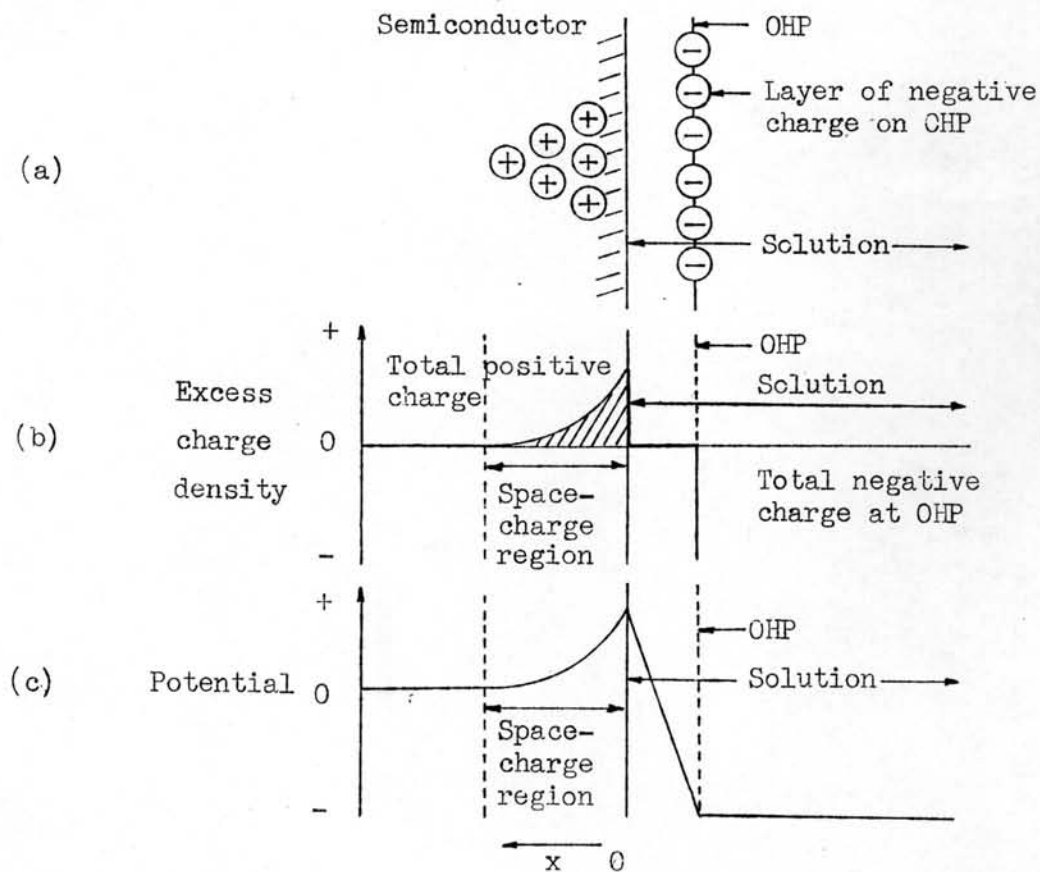


Figure 3.3.3 (a) The space charge inside a semiconductor, (b) the corresponding charge-density, and (c) the potential variation.

temperature. The term κ^{-1} was the measure of the thickness of the Garrett-Brattain space charge inside a semiconductor. The value of κ^{-1} diminished as the bulk concentration of charge carriers increased, such as by photoeffect.

In the solution, Band and Faulkner⁽⁶⁾ derived the equation for potential profile in the diffusion layer. From Gauss's law, this charge was

$$q' = \epsilon \epsilon_0 \oint_{\text{surface}} \mathcal{E} \cdot d\mathbf{s}$$

in Gaussian surface, the shape of a box placed in the system, \mathcal{E} , electric field was zero at all points on the surface except the end at interface.

(Figure 3.3.4)

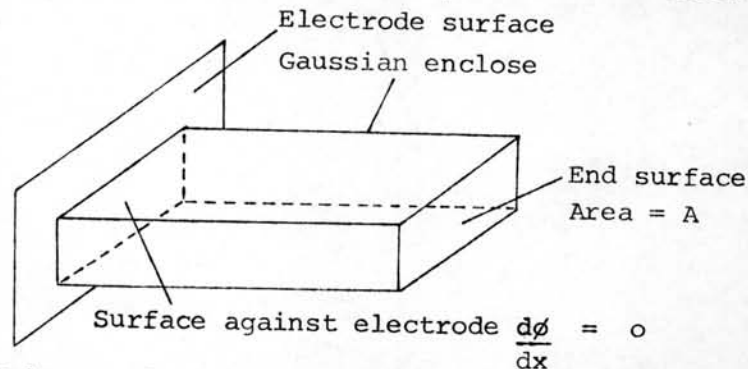


Figure.3.3.4A Gaussian box enclosing the charge in the diffuse layer opposite an area A of the electrode surface.

$$q' = \epsilon \epsilon_0 A \left(\frac{d\phi}{dx} \right)_{x=0}$$

The potential profile of diffusion layer was discussed and given⁽⁶⁾

$$\frac{d\phi}{dx} = - \left(\frac{8kTn_0}{\epsilon \epsilon_0} \right) \sinh \left(\frac{zq\phi}{2kT} \right)$$

where ϵ_0 and z were the permittivity of free space and the magnitude of the charge on the ions.

The solution space charge density σ^S , was q'/A term, thus

$$\sigma^S = \left(8kT \epsilon \epsilon_0 n_0 \right)^{1/2} \sinh \left(\frac{zq\phi_0}{2kT} \right)$$

where ϕ_o was related monotonically to the state of charge on the electrode.

Therefore, the capacity measurement were carried out on a semiconductor-electrolyte interface, the differential capacity could be calculated.

$$C_{SC} = \frac{d\sigma^s}{d\phi_o} = \left(\frac{2z^2 q^2 \epsilon \epsilon_o n_o}{kT} \right)^{1/2} \cosh(zq\phi_o/2kT) \dots 3.3.2a$$

They have modified Eq 3.3.2a to apply the surface diffusion layer of the n-type semiconductor and reduced some terms in the equation(3.3.2a) then became (6)

$$C_{SC} = \left(\frac{2 \epsilon \epsilon_o N_D}{2kT} \right)^{1/2} \left(- \frac{q\Delta\phi}{kT} - 1 \right)^{1/2}$$

Rearrangement of this equation yields was called the Mott-Schottky equation.

$$\frac{1}{C_{SC}^2} = \left(\frac{2}{q\epsilon\epsilon_o N_D} \right) (-\Delta\phi - kT/q) \dots 3.3.2b$$

where $-\Delta\phi = E - E_{fb}$, E , E_{fb} were the potential and the flat band potential, potential at which the semiconductor bands are flat. The application of this equation, a plot of $1/C_{SC}^2$ vs. potential, E should be linear, and the slope could be used to obtain the doping level N_D (donor atoms), and its interception also be used to obtain the flat band potential.

The flat band potential is the potential at which there is no excess charge in the semiconductor in the region of the semiconductor-solution interface, i.e. the conduction where there is no band-bending in the semiconductor. The Eq.3.3.2b was used for estimation of the flat band potential and donor or carrier concentration of semiconductor electrodes by many investigators (3,10,46,95,98)

3.4 Photoeffects at Semiconductor electrodes

3.4.1 Redox Reactions and Energy levels.

The fundamental postulate of semiconductor electrochemistry is that electron transfer occurs only at the bottom of the conduction band and top of the valence band. Thus, it is a knowledge of energy levels of these band positions at the surface of the semiconductor, relative to the energies of the reduced and oxidation from of the solution redox couple, that is required for a description of the transfer kinetics.

A clear picture of the relations of the energy bands in these semiconductors to the redox levels in the solution should explain this situation. In solid-state semiconductor measurements the energy bands are positioned relative to vacuum (see 3.2), while the presence of a liquid electrolyte necessitates a different reference, namely, the saturated calomel electrode, SCE. As a guide, one may recall that SCE is at +0.24V from the normal hydrogen electrode NHE, while NHE is about 4.5 eV below vacuum, so that SCE is 4.74 V below vacuum. This situation is depicted in Figure 3.4.1. ^(36,6)

	E (V vs.NHE)	E (V vs.SCE)	E (eV)
$E^{\circ}(\text{Cr}^{3+}/\text{Cr}^{2+})$	-0.41	-0.65	-4.09
NHE	0.00	-0.24	-4.5
SCE	+0.24	0.00	-4.74
$E^{\circ}(\text{Fe}^{3+}/\text{Fe}^{2+})$	+0.77	+0.53	-5.27
$E^{\circ}(\text{O}_2/\text{H}_2\text{O})$	+1.23	+0.99	-5.73

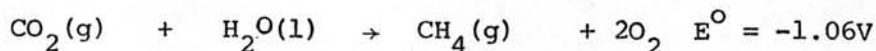
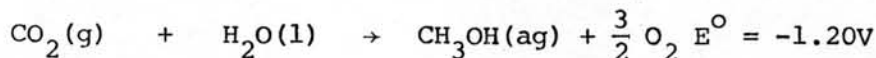
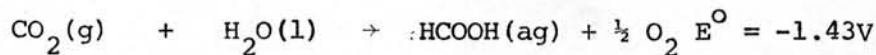
Figure 3.4.1 Relationship between potential scales based on the NHE, the SCE and the vacuum level.

Considering the fuel generation reactions in Table 2.1.3 as the redox reactions which have the potential energy (ΔE°) or the standard redox potentials (E°_{rxn} in Appendix A.3), the corresponding free energy change (ΔG°) as

$$E^\circ = \Delta G^\circ/nF \quad \dots 3.4.1.$$

where n is the number of electrons passed per atom of reactant component reacted and F is the charge on a mole of electrons. The ΔE° values in the Table 2.1.3 are calculated from Eq. 3.4.1, and the potentials are with respect to NHE.

Therefore a fuel production by photoelectrochemical cell, choosing electrode materials will be photoelectrode, their energy band levels and the redox potential of fuel product are considered at first. Figure 2.2.3a showed a comparison of the energy band of several of the semiconductors with the half redox potentials for the fuel reactions in Table 2.1.3. Both the band potentials of semiconductors and the redox reactions, the scales have the NHE as reference. Thus, the suitable overlap between the conduction bands and the redox potentials should be a choice of the material selection using in photocell for fuel production. For example, the reduction of carbon dioxide⁽²⁾ to formic acid, formaldehyde and methanol, their redox potentials were -0.20V of $\text{CO}_2/\text{HCO}_2\text{H}$, -0.07V of $\text{CO}_2/\text{H}_2\text{CO}$, + 0.03V of $\text{CO}_2/\text{CH}_3\text{OH}$ and + 0.17V of CO_2/CH_4 . The overall reactions are



and $\text{H}_2\text{O}(l) \rightarrow \frac{1}{2} \text{O}_2(g) + \text{H}_2(g)$ $E^{\circ} = 1.23\text{V}$. All of redox potentials of reduction carbon dioxide were estimated by the difference potential of a above reaction (or Table 2.1.3) and water splitting reaction, see Appendix A.3

Comparison of the energy bands and the redox potentials (Figure 3.4) indicated poor overlap between the conduction bands and the redox potentials, therefore the yield of product and quantum efficiency were low. For example, the quantum efficiency of $\text{CO}_2/\text{CH}_2\text{OH}$ reaction is shown in Figure 2.2.3 b, where the $\text{CO}_2/\text{CH}_2\text{OH}$ potential is -0.3V . The good overlap, the potential must be located at lower of level of conduction band (Figure 2.2.3a), the efficiency of WO_3 semiconductor was low according to the conduction band located near the potential. Note that the half reaction potential of $\text{CO}_2/\text{CH}_2\text{OH}$ is $+0.03\text{V}$ for the carbon reduction by above reaction, while it is -0.03V (Figure 2.2.3b) for the reduction by the reaction equation in section 2.2.3.

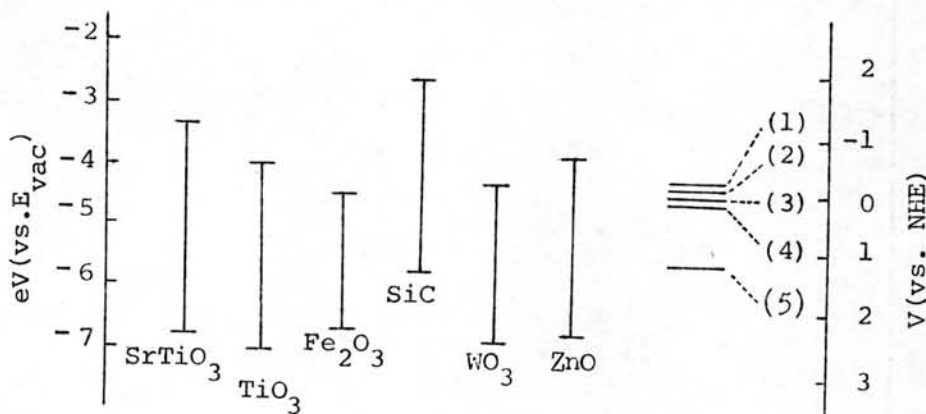
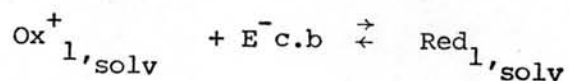
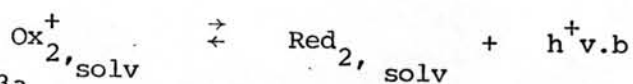


Figure 3.4 Comparison of widths and place of band gaps of various semiconductors with the redox potentials of interest in the carbon dioxide reduction : (1) $\text{CO}_2/\text{HCO}_2\text{H}$; (2) $\text{CO}_2/\text{H}_2\text{CO}$; (3) $\text{CO}_2/\text{CH}_3\text{OH}$; (4) CO_2/CH_4 and (5) $\text{H}_2\text{O}/\text{O}_2$, $E^{\circ} = -0.20, -0.07, +0.03, +0.17$ and $+1.23\text{V}$ respectively. (2)

There are two possible reactions occurring at the surface of a semiconductor. They have been shown that they depends on the particular redox system and on the individual semiconductor whether a redox reaction proceeds preferentially via the conduction or valence band⁽¹⁰⁾ The consequent formulation of a redox reaction at a semiconductor electrode with electrons (e^-) and holes (h^+) is therefore,



or



as Figure 3.4.3a

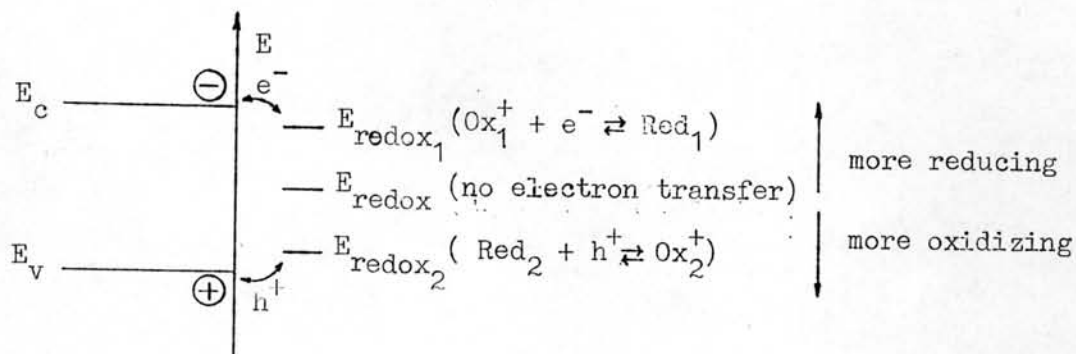


Figure 3.4.3a Energy correlations between semiconductor and redox couples in solution controlling electron exchange.

For example in the water decomposition, a suitable semiconductor has been shown in Figure 3.4.3b

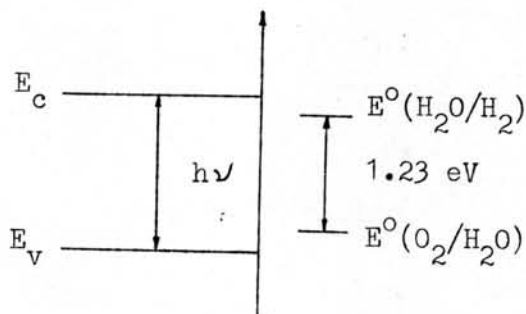


Figure 3.4.3b Conditions for the position of energy levels in order to allow water decomposition

The suitable semiconductor must have E_g which exceeds the redox potential at least 0.4-0.6 eV⁽⁵⁾, the discussion is in the next section.

In the simple case for photoelectrochemical cells, one electrode as photoelectrode is a semiconductor electrode and the other is always a metal as counter electrode. For the understanding of processes in cells, the electrochemical reaction at metal must be discussed too.

In an electrolysis cell, the counter electrodes are metals (e.g. Pt, Pd) and the redox reactions are controlled by the potential at each electrode. By driving the electrode to more negative potentials the energy of the electrons is raised, and they will eventually reach a level high enough to occupy vacant states on species in the electrolyte. In this case, a flow of electrons from electrode to solution (a reduction current) occurs (Figure 3.4.4a). Similarly, the energy of the electrons can be lowered by imposing a more positive potential, and at some point electrons on solutes in the electrolyte will find a more favorable energy on the electrode and will transfer there. Their flow, from solution to electrode, is an oxidation current (Figure 3.4.4b). The critical potentials at which these processes occur are related to the standard potential (E°), for the specific chemical substances in the system⁽⁵⁾.

In general, when the potential of an electrode is moved from its equilibrium (or its zero-current, value toward more negative potentials, the substance that will be reduced first (assuming all possible electrode reactions are rapid) is the oxidant in the couple with the least negative (or more positive) E° . For example, for a platinum electrode immersed in an aqueous solution containing 0.01 M each of Fe^{3+} , Sn^{4+} , and Ni^{2+} , in 1M HCl, the first substance reduced will be Fe^{3+} , since the E° of this

couple is most positive (i.e., Fe^{3+} is easiest to reduce) (Figure 3.4.5). Therefore, water electrolysis using platinum electrodes must avoid the Sn^{4+} and Fe^{3+} ions in the electrolyte.

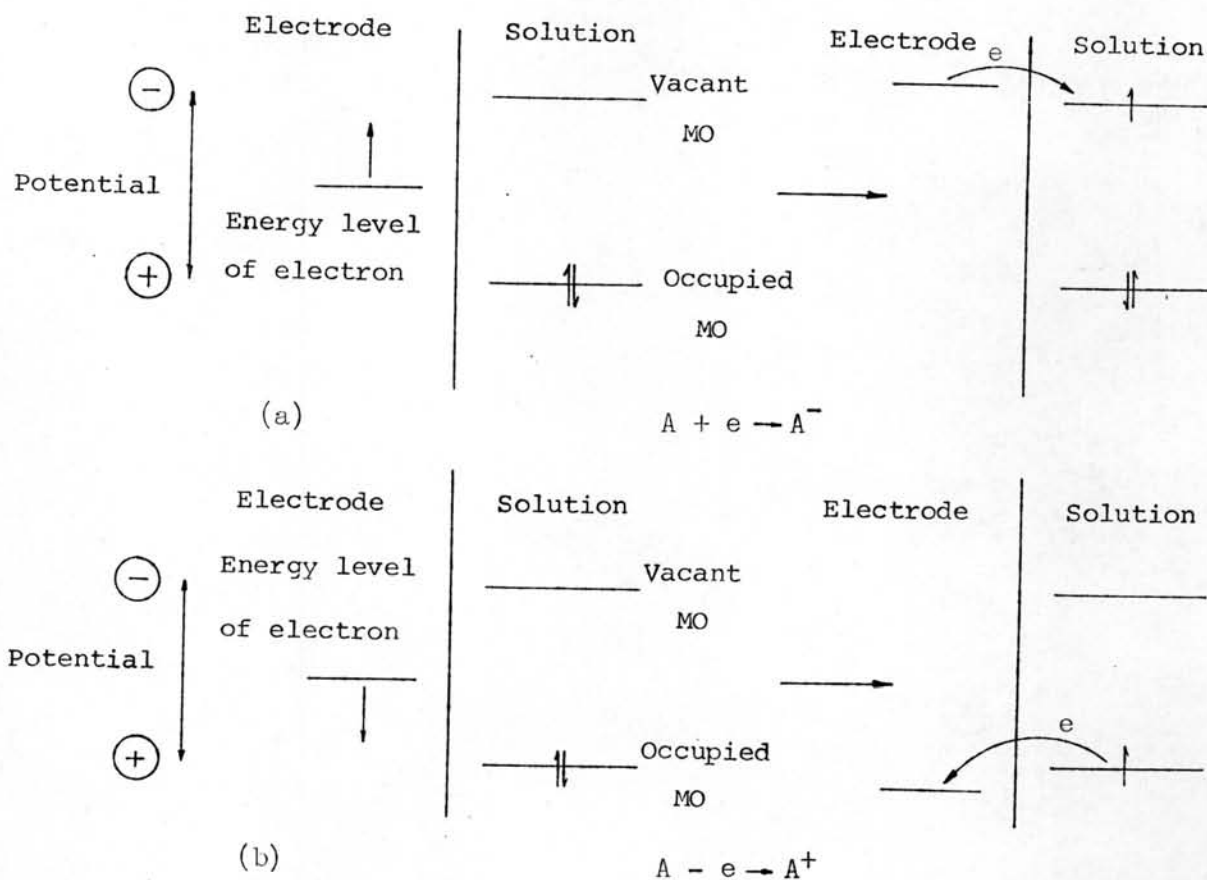


Figure 3.4.4 Representation of (a) reduction and (b) oxidation process of a species A in the solution. The molecular orbitals (MO) of species A shown are the highest occupied MO and the lowest vacant MO. As shown, these correspond in an approximate way to the E° 's of the A/A^- and A^+/A couples respectively.

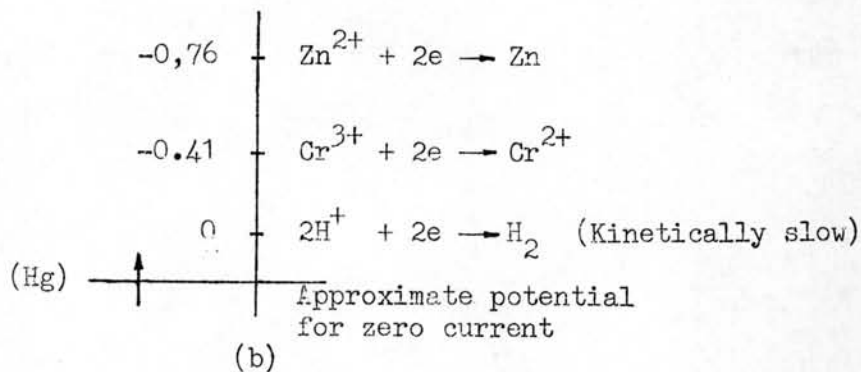
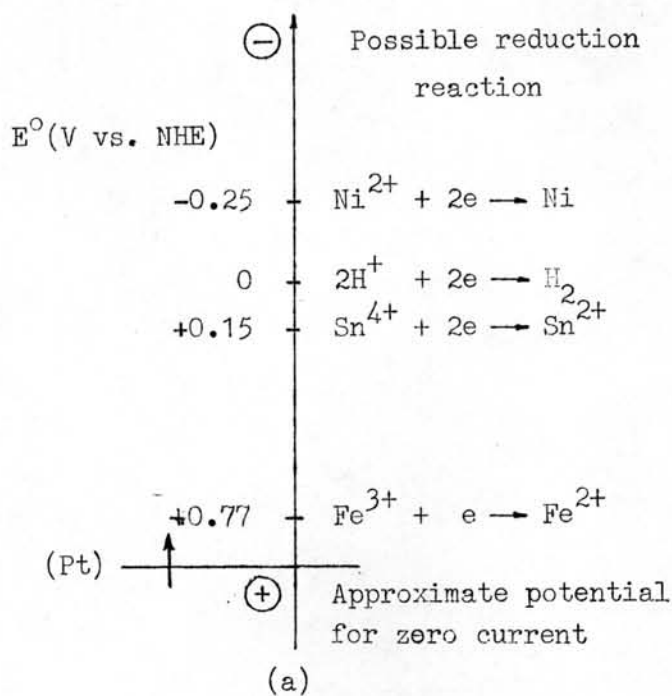


Figure 3.4.5 Potentials for possible reductions at platinum and mercury electrodes in 1 M HCl.

For a mercury electrode immersed in solution of 0.01 M each of Cr^{3+} and Zn^{3+} , 1 M HCl, the first reduction process predicted would be the reduction of H^+ (Figure 3.4.5b). This reaction is very slow on mercury. Therefore, these predictions are based on thermodynamic and kinetic consideration.

an important characteristic of Metal as electrodes in a electrolytic cell to be considered is the polarizability. From Figure 2.2. 1c, it shows the polarization characteristics of hydrogen electrolysis cell (its electrode is palladium), which the dotted line is the dissociation potential of water (1.23V). The curve is the d.c voltage vs. the current supplied to the cell.

The extent of polarization is measured by the overpotential, η , which is the deviation of the potential from the equilibrium value:

$$\eta = E - E_{eq} \dots\dots\dots 3.4.2$$

The resistance of the interface to the charge-transfer reaction caused the overpotential in the cell. The reaction resistance, which mainly depends upon the exchange current density, i_0 , at equilibrium⁽⁹⁾, determines what may be termed the polarizability, i.e., what overpotential a particular current density needs for a driven cell) of produces.

For hydrogen-evolution reaction, the measurement of the exchange current density gives a general ideal of the reaction rate in the standard state of equilibrium and permits the classification of the substrate upon which the reaction is occurring as a good or bad electrocatalyst electrode in the electrolytic cell. From Table 3.4.1, thallium and lead are poor catalysts for hydrogen evolution, and palladium and platinum are good and have values of exchange current densities in the milliampere range.

Table 3.4.1 The Exchange Current Density for the Hydrogen-Evolution Reaction. (9)

Metal	$-\log i_0$ (amp cm ⁻²) in 1M H ₂ SO ₄
Palladium	3.0
Platinum	3.1
Rhodium	3.6
Nickel	5.2
Gold	5.4
Tungsten	5.9
Silver	6.1
Titanium	8.2
Cadmium	10.8
Thallium	11.0
Lead	12.0

3.4.2 Photoprocesses at Semiconductor Electrodes.

Consider the formation of the junction between an n-type semiconductor and a solution containing a redox couple O/R, as shown in Figure 3.4.2.

In the dark, the junction formation (Figure 3.4.2. a and b) is similar to the Schottky junction of metal and semiconductor (Figure 3.2.2a and b), and the

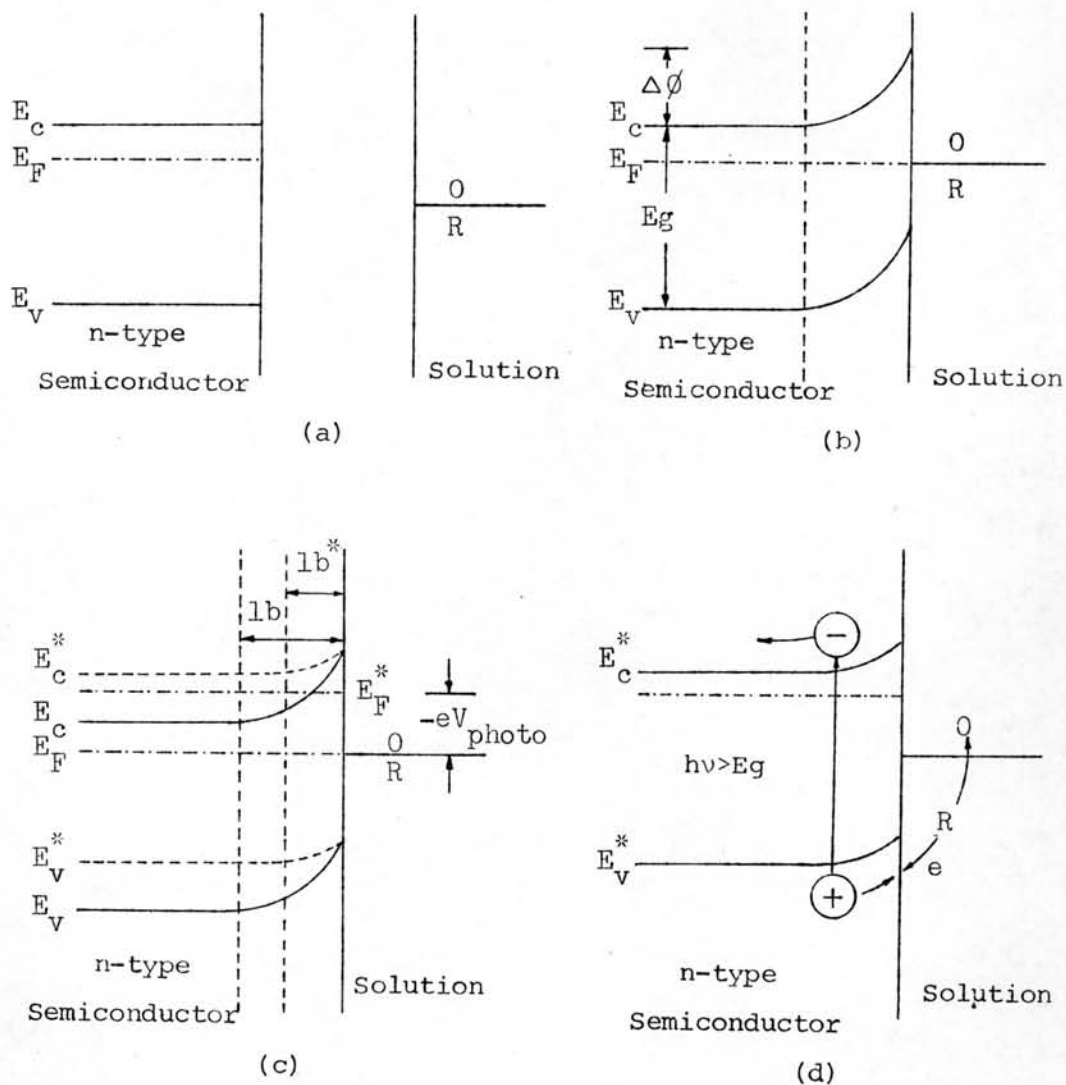


Figure 3.4.2 Representation of the formation of the junction between an n-type semiconductor and a solution. (a) Before contact in the dark. (b) After contact in dark and electrostatic equilibrium (c) Energy correlation in depletion layer for conduction band edge (E_c), valence band edge (E_v), and Fermi level (E_F) in the dark (E) and under illumination (E^*), and the space-charge layer (lb) in dark and under illumination (lb^*) (d) Reaction at the junction under illumination.

phenomena at the junction has been discussed in 3.3.2. Under illumination, the electric field, which was present in the space charge layer at equilibrium conditions, is disturbed by the process of charge separation. The electron-hole pairs which are generated within this layer (or reach this region by diffusion) are separated by the electric field, this drives the minority carriers (holes for n-type semiconductor) to the surface and the majority carriers (electrons) to the bulk of the semiconductor (Figure 3.2.2 d). In this case, the semiconductor-electrolyte biased by light is like the forward-biased metal-semiconductor junction ($\phi_m > \phi_s$), the barrier potential across the junction is smaller than in equilibrium, and causes the space-charge layer (lb) less narrow, too (Figure 3.4.2 c). The energy levels are also shifted up from equilibrium by photobias, the Fermi energy level of semiconductor is above the O/R redox potential by the eV_{photo} of the light energy in Figure 3.4.2 c. Therefore, the oxidation reaction will occur at the interface of the semiconductor and electrolyte ($R + e \rightarrow O$), when the circuit is closed via a counter electrode immersed into the same solution (see the next section). Thus irradiation of an n-type semiconductor electrode promotes photo-oxidations (or cause a photoanodic current), and the electrode is the photoanode in a cell.

To understand and to describe the thermodynamics of redox reactions between electrons in the conduction band or holes in the valence band and redox species in solution, it is useful to attribute individual redox potentials to each of these electronic transitions. For carrier (hole or electron) concentration in a semiconductor by calculation on the basis of quantum mechanics, the concentration of electrons is ⁽³⁹⁾

$$n = N_c \cdot e^{-(E_c - E_F)/kT}$$

and holes is

$$p = N_v \cdot e^{-(E_F - E_v)/kT}$$

where N_c and N_v are the effective densities of states in the conduction and valence bands, respectively. Both N_c and N_v are proportional to $T^{3/2}$.

Therefore the Fermi energy levels of electron and hole is from Eq.3.4a and b by arrangement as follow:

$$nE_F = E_c + kT \ln \left(\frac{n}{N_c} \right) \quad \dots 3.4a$$

$$pE_F = E_v + kT \ln \left(\frac{p}{N_v} \right) \quad \dots 3.4b$$

At equilibrium the Fermi levels of electrons and holes coincide due to the equilibrium condition as stated in Eq.3.1 or Eq.3.4c

$$n_0 p_0 = N_c N_v \exp \left(\frac{-E_c - E_v}{kT} \right) \quad \dots 3.4c$$

and

$$nE_F = pE_F \text{ if } n = n_0 \text{ and } p = p_0 \quad \dots 3.4d$$

Under illumination, in the steady state where generation and annihilation of electrons and holes compensate each other one has a concentration increase of Δn and Δp distributed in some way over space. By inserting the values at the surface for $n + \Delta n$ in Eq.3.4a and $p + \Delta p$ in Eq.3.4b, one obtains the individual redox potentials of electrons and holes which are effective at the electrode in the steady state of illumination or the so-called quasi-Fermi energies E_F^* (Figure 3.2.2. c). The logarithmic dependence of the Fermi level in Eq.3.4a and b gives for the shift of the quasi-Fermi levels of electrons or holes the following two equations: (11)

$$nE_F^* = nE_F + \Delta nE_F$$

$$\Delta n E_F = kT \ln \frac{(n_0 + \Delta n)}{n_0} \approx kT \ln \left(\frac{\Delta n}{n_0} \right) \text{ if } \Delta n \gg n_0 \dots 3.4e$$

$$p E_F^* = p E_F + \Delta p E_F;$$

$$\Delta p E_F = -kT \ln \frac{(p_0 + \Delta p)}{p_0} \approx -kT \ln \left(\frac{\Delta p}{p_0} \right) \text{ if } \Delta p \gg p_0 \dots 3.4f$$

The Eq. 3.4e and f are most important for estimating the maximum free energy which can be gained from an illuminated semiconductor electrode. This is indicated in Figure 3.2.3 by a shift of the quasi-Fermi level ($n E_F^*$ and $p E_F^*$) in the bulk of the n-type semiconductor relative to the water decomposition energy levels (Figure 3.4.3.b) in the solution under variable light intensity.

For example, n-type semiconductor in 3.1.2, N_D is about 10^{16} cm^{-3} and under equilibrium conditions ni^2 is about 10^{20} cm^{-6} . The majority carrier concentration, n_0 is approximately equals the donor concentration, 10^{16} cm^{-3} . Therefore the hole concentration is about 10^4 cm^{-3} (ni^2/N_D , see 3.1.2). The electron-hole pairs are formed by photo-excitation, they give the magnitude of the change in the concentration of electrons the same as the change in the concentration of holes, $\Delta n = \Delta p$. If Δn is about 10^{12} cm^{-3} , the excess carrier concentration will be negligible small in comparison to the doping concentration. Thus, by representing n_0 with N_D in Eq. 3.4e the $\Delta n E_F$ will be small because of $\Delta n \ll N_D$, and in Eq. 3.4f the $\Delta p (10^{12} \text{ cm}^{-3})$ is much larger than $p_0 (10^4 \text{ cm}^{-3})$, the $\Delta n E_F$ will be large negative.

From Figure 3.4.3, at dark the $n E_F$ and $p E_F$ is located at the same level (by Eq. 3.4d), it is near the lower edge of conduction band (E_c) for an n-type semiconductor. Under moderate illumination, the divergence between the quasi-Fermi levels of electrons and holes increases from the

bulk to the surface while the quasi-Fermi level for the majority carriers (electrons), nE_F^* , remains practically constant with only a slight deviation close to the surface. The quasi-Fermi level of the minority carriers (holes), pE_F^* , deviates, therefore, more and more from its equilibrium value in the bulk and in the surface approaches the range of the band edge. In this case, $\Delta n = \Delta p \ll N_D$ is the condition of this process, ΔnE_F is very small so the nE_F^* is little shift level from nE_F at equilibrium, and ΔpE_F is very large negative, so the pE_F^* is much shift level from pE_F , too as Eq.3.4e and 3.4f.

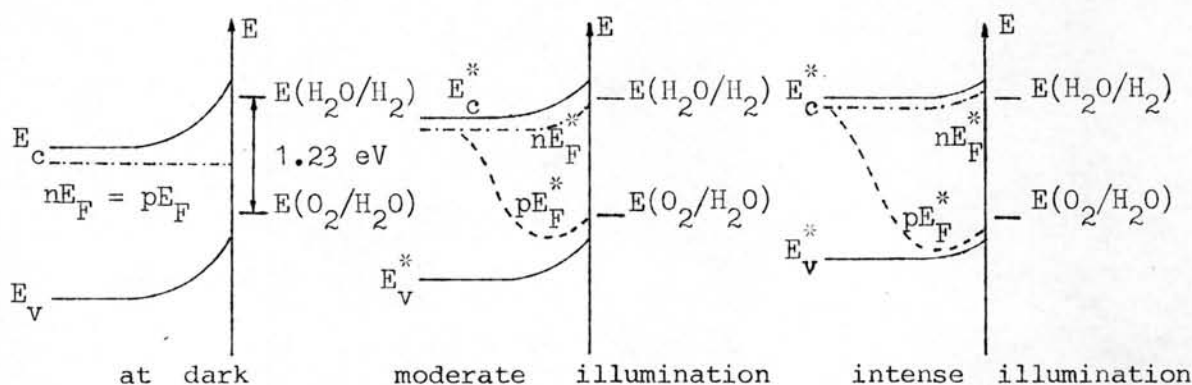


Figure 3.4.3 The quasi-Fermi levels of electrons and holes in an illuminated Schottky-barrier at the semiconductor-redox electrolyte interface suitable for water decomposition. (10)

The three cases in Figure 3.4.3 can be explained and compared with the injection of n-type silicon (Figure 3.4.4.) in the dark and under illumination. The behavior of the interface by moderate illumination, the excess carrier concentration is negligible small in comparison to N_D , i.e;

$\Delta n = \Delta p \ll N_D$, is referred to as low-level injection, and by intense illumination the hole and electron concentration more than N_D , is referred to as high-level injection

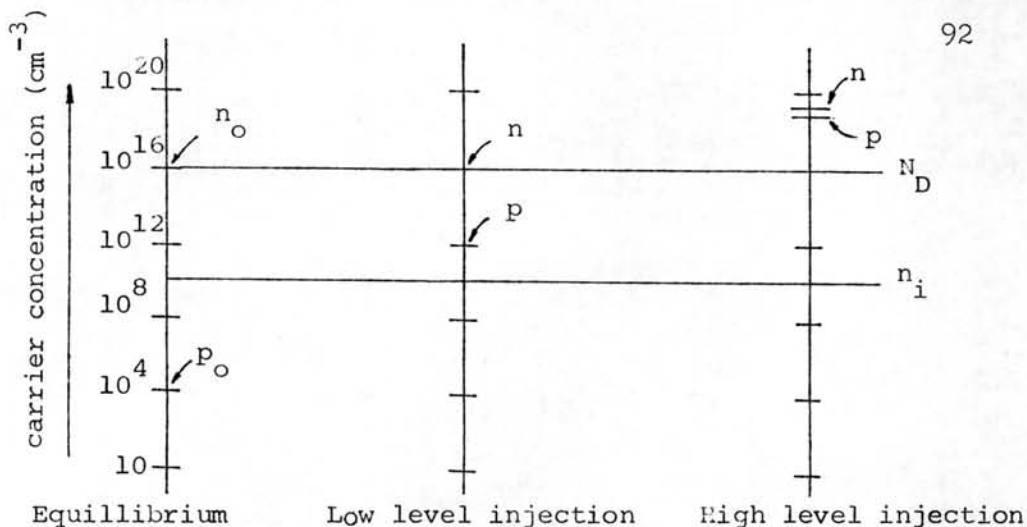


Figure 3.4.4 Illustration of the concentration of electrons and holes in an n-type in equilibrium and under low- and high-level injection (39)

Above phenomena shows again that the band gap of the semiconductor must exceed the decomposition voltage by a considerable amount, as is indicated in Figure.3.4. 3. The condition for the possibility of water decomposition at a suitable semiconductor surface is therefore : $nE_F^* > E(H_2O/H_2)$ and $pE_F^* < E(O_2/H_2O)$, or the shift energy level of nE_F^* and pE_F^* is greater than the difference of $E(H_2O/H_2)$ and $E(O_2/H_2)$, is 1.23 eV. The maximum value which can be reached for the photo-voltage (V_{photo}) is the flat band potential (see 3.3.2). Before this situation is reached, recombination will reduce the quantum yield so considerably that the efficiency for energy conversion decreases to an unacceptable low value.

For the reduction of carbon dioxide, the redox potentials is between the conduction and valence bands of SrTiO₃, TiO₂, ZnO and SiC (Figure 3.4.2), above the reason, the split of quasi-Fermi energy level shows the SiC should be a good photocatalyst for this propose (50) because of the good overlape the redox reaction and the conduction band. Thus, TiO₂ and ZnO should be photocatalyst for the same efficieney but in

practice, ZnO is bad, according to its instability in solution for this process under illumination. The stability of materials is an important characteristic for choosing the suitable catalyst or electrode material.

3.4.3 The Stability of Illuminated Semiconductors

The stabilization of the semiconductor photoanodes by redox agent have been studied in the semiconductor/electrolyte system by many investigators. (7,32,85) There are some conditions of the system to be considered for stability of electrode such as the redox potential, (32) pH (83) the decomposition potential of semiconductor, (7) E_D , the electrolyte substance and surface state (55).

For example, comparison of TiO_2 , CdS and ZnO electrodes are used for water photoelectrolysis. The important parameter is the E_D of them, as follow:

Reaction	E_D (V v.s. NHE) at pH 0
$CdS \rightarrow Cd^{2+} + S + 2e^-$	+0.32
$ZnO \rightarrow Zn^{2+} + \frac{1}{2} O_2 + 2e^-$	+0.89
$TiO_2 \rightarrow TiO + \frac{1}{2} O_2 + 2e^-$	+1.41

In this case, the TiO_2 photoanode is a stable electrode because its decomposition potential is greater than the redox potential of water decomposition (+1.23V), while CdS and ZnO are smaller so they are easily oxidised for small potentials, 0.32 and 0.89 V (Figure.3.4.5).

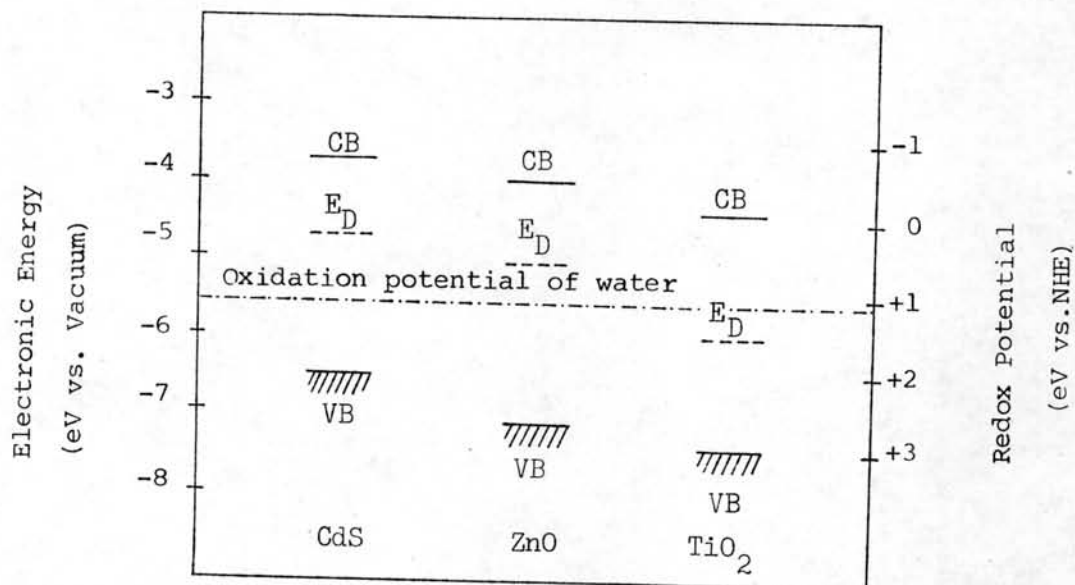


Figure 3.4.5 Energy position of band edges of CdS, ZnO and TiO_2 in relation to the redox potential for water decomposition

For a stable TiO_2 electrode, Harris⁽⁴⁵⁾ found that the TiO_2 crystal photoanode was corroded slightly in sulfuric acid solution, and they prevented this corrosion by adding some cobaltous ions in electrolyte (0.5 M H_2SO_4).

From many experiment results, semiconductors with the large band gap energy are always stable for water decomposition, the small band gap energy are unstable, as shown in Table 3.4.3.

Table 3.4.3 Semiconductors tested as Electrodes for
Photodecomposition of Water⁽³⁶⁾.

Material	E _g (eV)	Remarks
Si	1.1	corrodes
GaAs	1.4	"
CdSe	1.7	"
GaP	2.2	p-GaP is stable (92)
CdO	2.3	no response
CdS	2.4	corrodes
WO ₃	2.7	stable at low pH.
TiO ₂	3.0	stable
SiC	3.0	corrodes
SrTiO ₃	3.2	stable
ZnO	3.2	corrodes
Nb ₂ O ₅	3.4	stable
SnO ₂	3.5	stable

3.5 Semiconductor Electrodes in Photoelectrochemical Cells.

In photo electrochemical cells, one semiconductor is an a electrode and the other electrode is called a counter electrode, e.g. platinum. The contact between as illuminated semiconductor electrode has the great advantage that it is easy to transfer the electrons to an electrode with good catalytic properties so that there the respective electrode reaction can occur with very low overvoltage. There are three types of photoelectrochemical cells (PEC's), as shown in Figure 1.2.2 For conversion of sunlight energy application, two important types will be discussed in this section. PEC's for chemical synthesis is known as photoelectrosynthetic cells. Water decomposition for hydrogen production is a interesting conversion of solar energy by PEC's, such a cell is schematically outlined in Figure 3.5.1

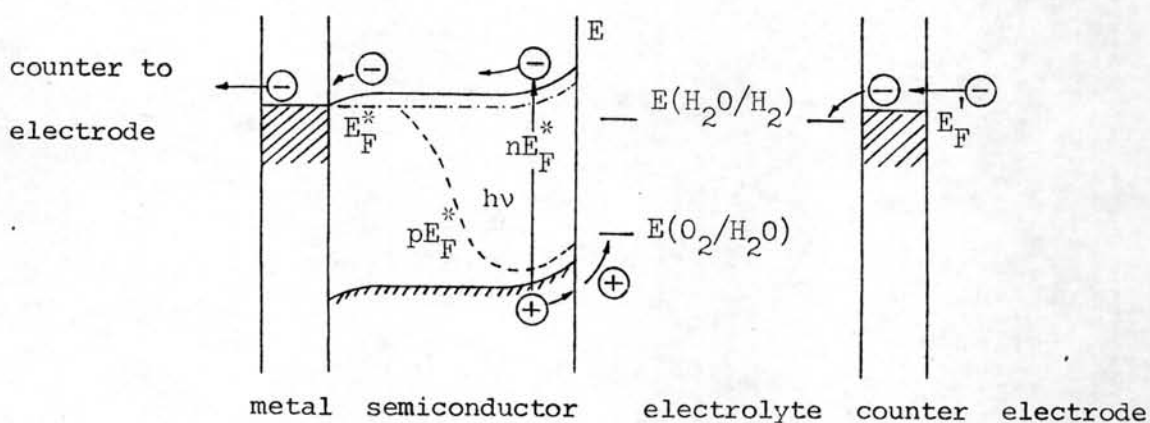


Figure 3.5.1 A photoelectrochemical cell for water decomposition with catalytic counter electrode.

The other type is called as photovoltaic cell (or photoelectrolytic cell) for solar energy conversion to electrical energy. The regenerative operation of a photovoltaic cell, electrochemical reaction proceeding at the semiconductor electrode in one direction must be fully compensated by

the same reaction at the counter electrode proceeding in the opposite direction. If this condition is fulfilled, no chemical change will occur in the electrolytic cell (in Appendix A.3). Such cells, an n-type semiconductor in contact with a redox electrolyte is shown in Figure 3.5.2, and p-type semiconductor is shown in Figure 3.5.3.

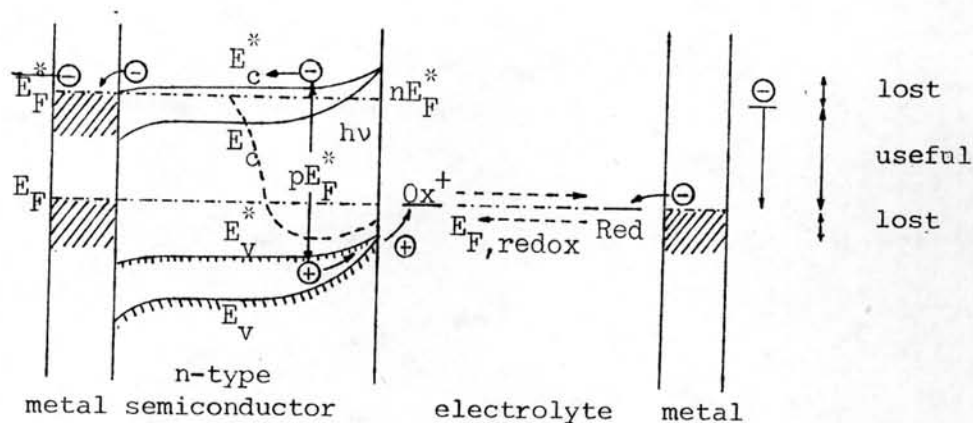


Figure 3.5.2 Photovoltaic cell operating in the regenerative mode as power source with an n-type semiconductor as anode.

The contact between the semiconductor and electrolyte must form a Schottky-barrier in the absence of illumination. This can be achieved by using a suitable redox system since its redox potential controls the position of the Fermi level of the electrode in the equilibrium situation in the dark. In the n-type semiconductor, the redox Fermi level in the electrolyte must be located as close as possible to the conduction band edge which is necessary for obtaining large photovoltages. For a p-type semiconductor one has to meet the opposite conditions and the redox Fermi level of the electrolyte should be located close to the valence band edge.

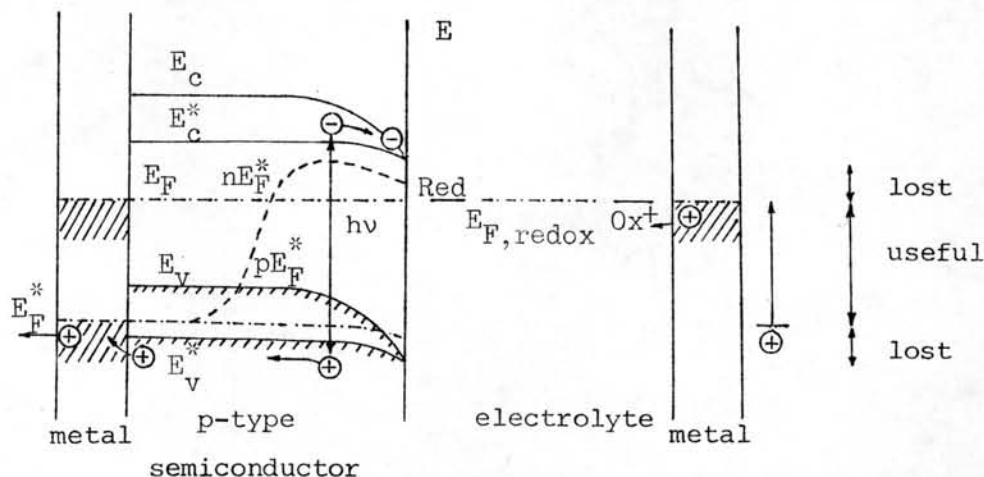


Figure 3.5.3 Photovoltaic cell operating in the regenerative mode as power source with a p-type semiconductor as cathode

If such the system is illumination a current flows immediately from the illuminated electrode to the counter electrode, carried by the majority carriers (electrons for n-type and holes for p-type) of the semiconductor, while the minority carriers (holes for n-type and electrons of p-type) reach the semiconductor-electrolyte interface (Figure 3.5.2 and 3) The n-type semiconductor needs a positive excess charge and a space charge layer depleted of electrons is formed at potentials positive from the flat band potential, this the band is bent up, and under illumination the energy level also change as explained previously. The holes from valence band (Figure 3.5.2) oxidize the redox system at the semiconductor which has to be stable against photooxidation. The electrons after having reached the counter electrode reduce there the same redox system so that the net chemical change in the electrolyte is zero. For the p-type semiconductor has a space charge layer depleted of holes at a potential negative from the flat band potential, so the band is bent down. Under illumination, according to $\Delta p \ll p_0$ and $\Delta n \gg n_0$ for Eq. vii and viii, therefore nE_F^* will shift up from the

E_F at equilibrium widely, while pF_F^* will slightly shift (Figure.3.5.3). The electrons from the conduction band reduce the redox system at semiconductor which has to be stable against photoreduction. The photo-generated holes are transferred to the counter electrode where they oxidise the redox system.

Therefore the photovoltage generated between the semiconductor electrode and the counter electrode can be used, for work (see 3.5.2). For the photoelectrosynthetic cell more discussion of details for the water decomposition case will be discussed in chapter IV.

3.5.1 Some Theory of the Semiconductor-Electrolyte Interface as a Schottky Barrier

The semiconductor-electrolyte interface is considered to behave in a manner analogous to a metal-semiconductor Schottky barrier, as explained previously. This view is taken because the solution is much more conducting than the solid phase, and therefore, essentially all of the depletion region falls within the semiconductor. If should therefore be possible to derive an expression relating the magnitude of the response of a cell to the wavelength of incident light, this has been done recently by Ghosh and Maruska for TiO_2 .^(36,59) Briefly, consider a semiconductor electrode of thickness l , with a depletion region of width l_b and a minority carrier (hole) diffusion length L . The number of photogenerated carriers (see 3.1.5) within dx at a distance x from the solution-semiconductor interface is proportional to (Eq.3.8)

$$\phi N \alpha \exp(-\alpha x) dx$$

where ϕ is the number of carrier pairs produced for each absorbed photon, N is the number of incident photons, and α is the absorption constant for

photons of this wavelength. The carriers produced in the bulk, at a distance x from the surface, will have a fraction proportional to

$$\exp - (x - lb)/L$$

diffuse to the edge of the barrier region. The others will recombine and be lost, it is assumed here that recombination in the barrier region may be neglected. Then the total number of holes contributing to the current, one generated in the barrier region and one due to diffusion from the bulk, so that

$$p = \phi N_0 \int_0^{lb} \alpha \exp(-\alpha x) dx + \phi N \int_{lb}^{\infty} \alpha \exp(-\alpha x) \exp -(x-lb)/L dx$$

The first term accounts for carriers generation in the barrier region and the second term is for carriers from the bulk. Therefore, the total photocurrent is given by

$$J = qNG \left[1 - \exp(-\alpha lb) + \frac{\alpha}{\alpha + \beta} \exp(\beta lb) \{ (\exp - (\alpha + \beta) lb) - (\exp - (\alpha + \beta) l) \} \right] \quad \dots\dots\dots 3.5.1a$$

Here J is the photocurrent /cm² (current density) and $\beta = 1/L$. G is a factor related to the quantum efficiency ϕ , the photoconductive gain in the barrier region, and to the process governing the transport of holes across the interface.

Using the absorption spectrum for TiO₂ available to relate α and λ , Ghosh and Maruska⁽³⁶⁾ determined that there is a good fit of their experimental data with the relationship given in Eg.3.5.1a. According to the width of barrier region (or depletion layer thickness or the space charge region), lb , is related to the voltage or potential in this region (Figure 3.4.2c) is given by (36,59)

$$lb = \frac{(2\epsilon\epsilon_0 q^2)^{1/2}}{qN_D} (V - V_{fb})^{1/2}$$

or

$$l_b = W_0 (V - V_{fb})^{\frac{1}{2}} \quad \dots\dots\dots 4.5.1b$$

where $W_0 = (2\epsilon\epsilon_0/q N_D)^{\frac{1}{2}}$ (cf. A.1.4 of p-n junction), depletion layer thickness for 1V drop across space charge layer, V_{fb} is flat band potential, and N_D is the donor density for a n-type semiconductor. Under illumination with monochromatic light with $h\nu > E_g$, a photocurrent is given by Butler and Ginley, who obtained

$$j = q\phi_0 \left\{ 1 - \frac{\exp[-\alpha W_0 (V - V_{fb})^{\frac{1}{2}}]}{1 + \alpha L_p} \right\} \quad \dots\dots\dots 3.5.1c$$

where q = electronic charge, ϕ_0 = photon flux of light, V = applied potential, L_p = hole diffusion length before recombination, Further, if $\alpha \cdot L_p$ is $\ll 1$, which is certainly true for $h\nu < E_g$, and roughly true for $h\nu > E_g$, then ⁽⁸⁵⁾

$$J = q\phi_0 \left\{ 1 - \exp[-\alpha W_0 (V - V_{fb})^{\frac{1}{2}}] \right\} \quad \dots\dots\dots 3.5.1d$$

For the photocurrent, J in Eq. 3.5.1c, agreement with experimental results is excellent at higher voltages, but deviations are found at small voltages, ⁽⁵⁸⁾ and the surface recombination ⁽⁷²⁾ is only important at small values of the voltage, near V_{fb} .

For example of a $I - V$ characteristic in the experiment for TiO_2 in acidic solution, in the dark and illuminated with 200 W Hg lamp, is shown in Figure. 4.2.1 in Chapter IV.

The potential for chemical reaction study in the solution of a photocell is always determined by measure the voltage of semiconductor with respect to electrolyte by SEC electrode. But the cell voltage through external circuit is that of the semiconductor with respect to the metal (Pt) and is positive when the semiconductor is the anode. The starting potential of the oxidation reaction at TiO_2 electrode corresponds almost exactly to the flatband potential which is constant in the electrolyte solution of a given pH.⁽³¹⁾ That may be explained by Eg. 4.5.1d, at $V = V_{fb}$ as the current density, $J = 0$, However this point, the voltage is not a exact flat band potential. Consider the detail of I-Vcurve of TiO_2 and SrTiO_3 ⁽⁵⁸⁾ electrodes and the energy diagram of their electrodes, the flat-band potential can be determined by the potential of the fermi level under intense illumination (Figure 3.5.6, light), because the flat-band potential is the potential at which there is no excess charge in the semiconductor in the region of the semiconductor-solution interface, i.e. the conduction where there is no band-bending in the semiconductor. Therefore, the starting potential ($I = 0$) of I-Vcurve (Figure 3.5.5) is -1.22 V for SrTiO_3 and -1.03V for TiO_2 , they are the potentials of the located Fermi level of electrons (nE_F^*) (Figure 3.5.6 light). Thus V_{fb} must be at least -1.03V for TiO_2 , and -1.22V for SrTiO_3 . This is a reason for water decomposition by TiO_2 with small bias from the external power while SrTiO_3 without any bias,^(94,95) because of the $nE_F^* < E_{\text{H}_2/\text{H}_2\text{O}}$ for TiO_2 electrode and the $nE_F^* > E_{\text{H}_2/\text{H}_2\text{O}}$ for SrTiO_3 electrode in Figure 3.5.6, light.

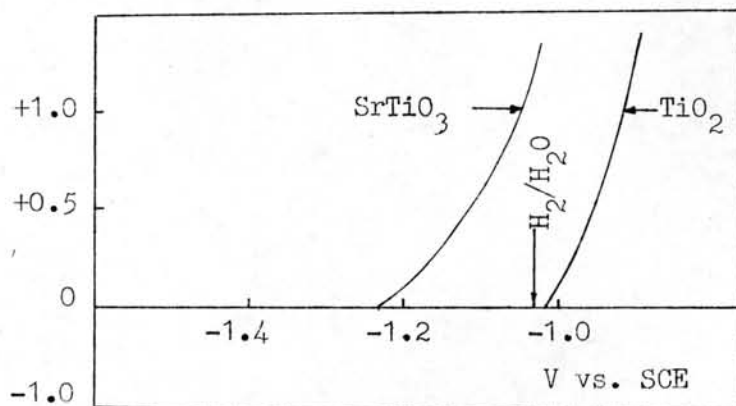


Figure 3.5.5 Details of the current-voltage characteristics of illuminated TiO_2 and SrTiO_3 electrodes in the potential region of the $\text{H}_2/\text{H}_2\text{O}$ redox couple (5M KOH solution) (59)

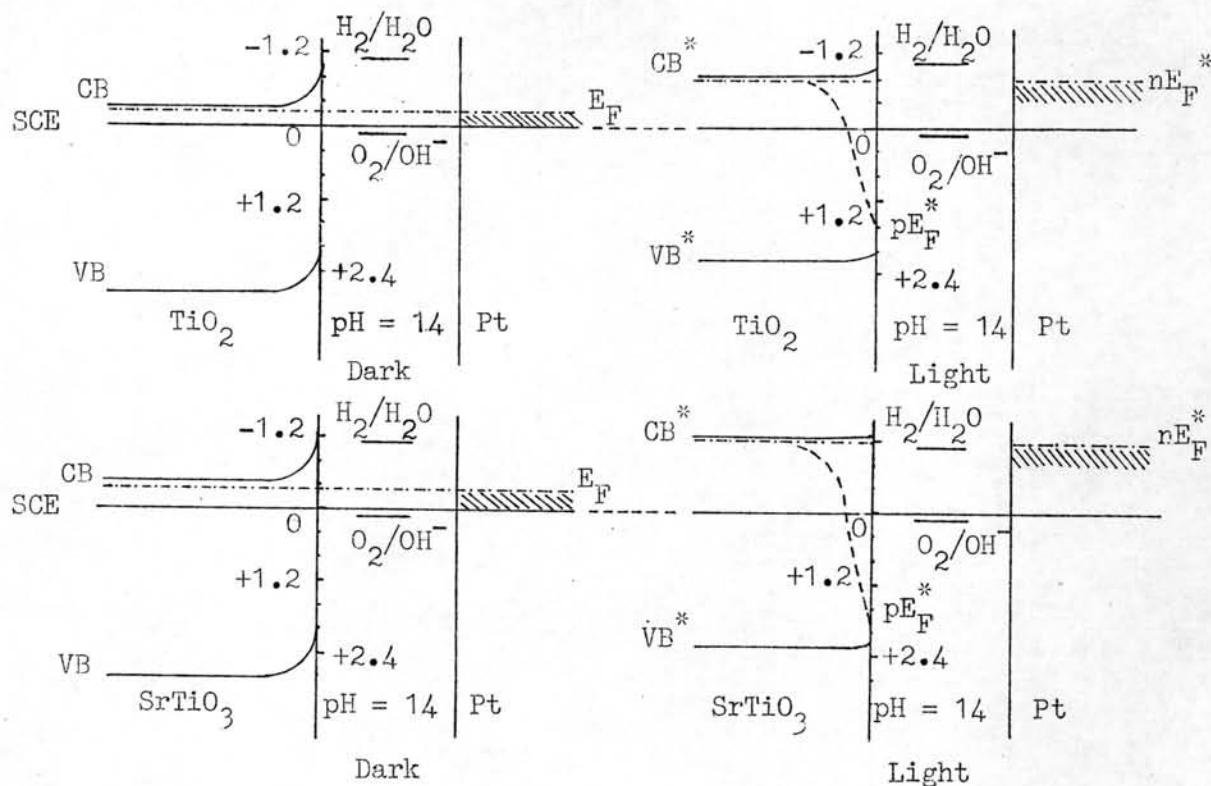
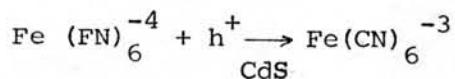


Figure 3.5.6 Energy level diagrams for TiO_2 and SrTiO_3 photoelectrochemical cells in the dark and under illumination. (59)

3.5.2 The Photovoltaic Cells

Up to now both n-type and p-type semiconductors seem to have been used this type of operation, as explained previously. The most studied

systems are the small band-gap semiconductors (e.g. CdS, CdSe, GaAs etc.) in contact with different redox electrolyte, in which the semiconductor electrodes are stable under illumination. For example, n-CdS electrode can be stabilized in ferri-ferrocyanide-solutions,⁽⁶⁵⁾ by the oxidation reaction;



The energy relation for this system is shown in Figure 4.5.7⁽¹⁰⁾

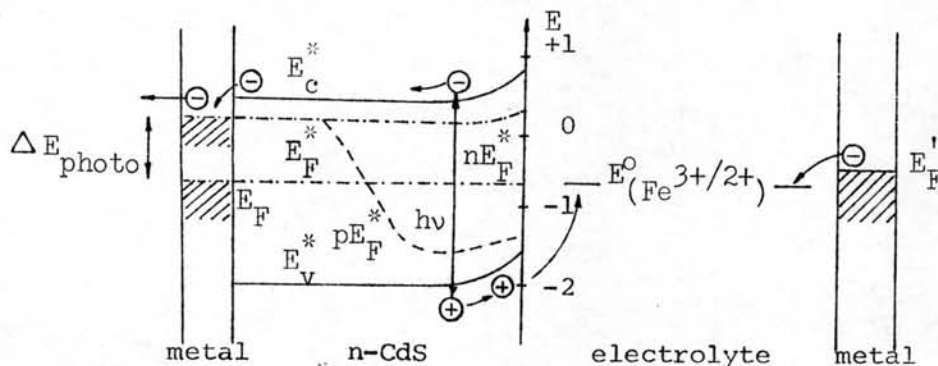


Figure 4.5.7 Regenerative photoelectrolytic cell with CdS-electrode and $\text{Fe}^{3+}/2+$ -redox system.

The obtainable photovoltage is controlled by the distance between the Fermi level of the redox system and the flat band potential of the semiconductor. The ferric/ferrous redox system should therefore be able to reach a photovoltage close to about 1.4 eV.⁽¹⁰⁾ In practice, the power characteristics of such a cadmium sulfide redox electrolyte solar cell are shown in Figure 4.5.8, the V_{OC} is about 1.22 V. At optimal load, a conversion efficiency was estimated about 6-7%, its calculation is like the solar cell efficiency (in Appendix A.2).

Several different figures of merit are conveniently used to represent various aspects of conversion efficiency :

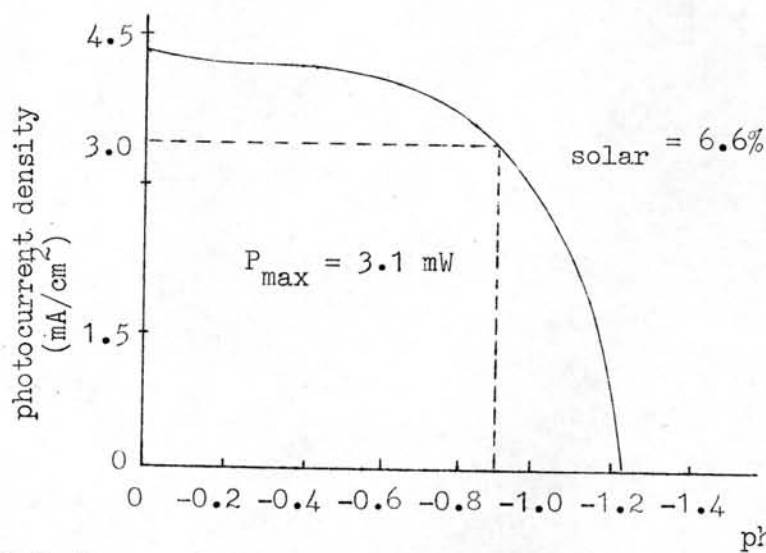


Fig.3.5.8 Power characteristic of CdS-redox electrolyte photocell with the ferri-ferrocyanide-redox (pH = 5.5) illumination with XBO 150 lamp. ⁽¹⁰⁾

i. Practical over all efficiency for conversion of solar energy is designated by sunlight engineering efficiency, S.E.E., Eq.3.5.2a where the power point is the maximum I.V product achievable by variation of load.

$$\text{S.E.E.} = \frac{\text{Electrical Power Delivered to Load at Power Point} \times 100}{\text{Incident Sunlight Power}} \quad \dots 3.5.2a$$

In an ideal photovoltaic or photogalvanic cell, the I.V product is insensitive to load and equals the product of the short circuit current, I_{sc} , times the open circuit voltage, V_{oc} (see Appendix A.2). The ratio (I.V) power point $I_{sc} \cdot V_{oc}$ is known as a fill factor.

ii. The overall efficiency for conversion of the power of absorbed photons into electrical power delivered to load, the quantum power efficiency, ϕ_p , is given by equation 3.5.2b.

$$\phi_p = \frac{\text{Electrical Power Delivered to External Circuit}}{\text{Absorbed Light Power}} \dots 3.5.2b$$

ϕ_p is a measure of the combined effects of wasting some of the photon which are absorbed and to the wastage of part of each photon which is utilized.

iii. The isolated number efficiency for conversion of photons, the quantum current efficiency, ϕ , is given by equation 3.5.2c.

$$\phi_i = \frac{\text{Number of Electrons Delivered to External Circuit}}{\text{Number of photons Absorbed}} \dots 3.5.2c$$

ϕ_i is a measure of the combined effects of wastage of absorbed photons in photophysical, photochemical and bulk ground state chemical processes.

For example, the quantum efficiency for photocurrent generation at chlorophyll electrodes in a photoelectrochemical cell (see 2.3.3.). The quantum efficiency, ϕ , at wavelength λ can be calculated by the following equation⁽⁶⁸⁾

$$\phi_\lambda = (I_{p\lambda} / q) / (F_{\text{abs}})_\lambda \dots 3.5.3d$$

where $I_{p\lambda}$ is the photocurrent (A cm^{-2}) at wavelength λ , q the elementary charge (1.6×10^{-19} coulombs), and $(F_{\text{abs}})_\lambda$ the number of photons ($\text{cm}^{-2} \text{s}^{-1}$) absorbed by the monolayer. $(F_{\text{abs}})_\lambda$ is calculated using the number of incident photon, $F_{i\lambda}$, and the absorbance, A_λ , of the monolayer in contact with the electrolyte solution, as follows:

$$(F_{\text{abs}})_\lambda = F_{i\lambda} (1 - 10^{-A_\lambda})$$

There are a few important photoelectrodes for photovoltaic cells of recent studies, such as CdS, CdSe and GaAs. They are always unstable in aqueous electrolyte, but in suitable electrolyte they are stable only as photoelectrodes of photovoltaic cells, not for photoelectrosynthetic cells.

The n-CdSe thin film photoanodes have been studied, they are stable in aqueous sulfide-polysulfide containing electrolytes. (48,80) There are two models, of thin-film photovoltaic cell designs frontwall cell and backwall cell (Figure 3.5.9). The CdSe thin films were produced by

the simultaneous evaporation of Cd and Se deposited onto titanium sheets for frontwall cell, the power conversion efficiency of these electrode was only in the range 3-4% at 75 mW/cm^2 , AM2 conditions.⁽⁸⁰⁾ The interesting feature of films produced in this manner was their higher open-circuit voltage, which was consistently in the range of 0.55 to 0.65 V. However, the current output and fill factor were low, because L_p , hole diffusion length was quite small ($<0.02 \mu\text{m}$) and other parameters

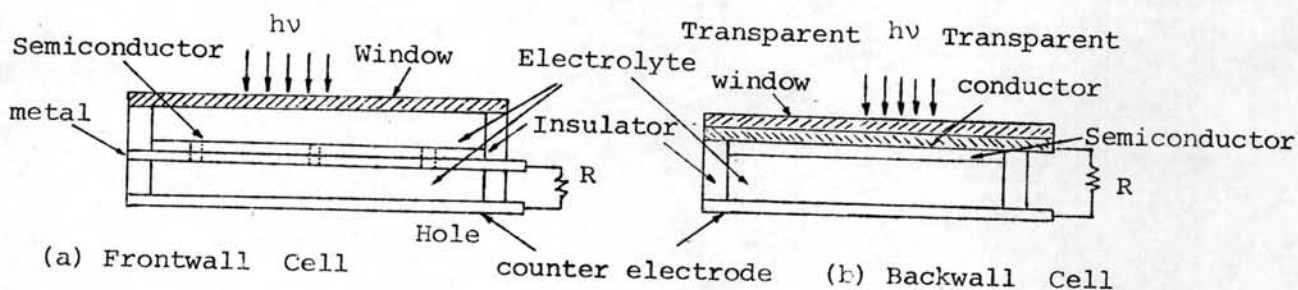


Figure 3.5.9 Thin-film photoelectrochemical cell designs.

characterize the losses due to recombination in the depletion region. For the backwall cell, CdSe thin film was deposited on SnO_2 coated glass slides for transparent electrode.⁽⁸¹⁾ The short-circuit current density was 17 mA/cm^2 and the open-circuit voltage was 0.45 V at 75 mW/cm^2 , AM 2. As a result, the power conversion efficiency was greater than 4% and fill factor was 0.42.

A interesting photoelectrode with high efficiency is a GaAs electrode.^(62,65) The n-GaAs was coated with metal films (e.g. Au, Pt, Rh) to protect corrosion. Under solar illumination ($69\text{-}90 \text{ mW/cm}^2$), the conversion efficiency of Au, Pt and Rh plated n-GaAs was 2-6% in ferro-ferricyanide solution.⁽⁶²⁾ Recently, Noufi and Tench⁽⁷³⁾ has studied n/n⁺-GaAs in aqueous selenide/polyselenide solution, compared with that of single crystal in photovoltaic cells. The designation n/n⁺ denotes a

layered structure of a lightly doped film deposited on a more heavily doped substrate of the same material. This structure can be formed both in ~~single and polycrystal~~ crystal. Characteristics of two cells are summarized in Table 3.5.2, These systems are under xenon lamp illumination from 250 to 885 nm.

Table 3.5.2 Characteristics of photoelectrochemical cells based on n/n^+ -GaAs in selenide/polyselenide solutions under illumination with light (115 mW/cm^2) from a xenon lamp. ⁽⁷³⁾

Parameter	Polycrystalline	Single crystal
Open-circuit voltage (V)	0.68	0.7
Short-circuit current (mA/cm^2)	29	29
Fiff factor	0.67	0.80
Maximum power output (mW/cm^2)	14	16
Power conversion efficiency		
Uncorrected	12%	14%
Corrected for solution		
absorption	16%	19%

Therefore, the further studies of small band gap semiconductors for photoelectrochemical cells or photovoltaic cells as solar cells should be widely investigated. The interesting manner of this cells is that the open-circuits are high voltage of 0.4-0.8 V, while the solid-state solar cells are about 0.5-0.6V. However, the power conversion efficiency of PCE's are still low, but in developed cells it should be possible to increase the efficiencies as high as silicon solar cells. Also,

Si is a semiconductor electrode of PEC's, recently Fan⁽²⁴⁾ has attempted to demonstrate the suitable system for Si electrode stabilized in PEC's.